Chemistry Africa (2022) 5:375–393
https://doi.org/10.1007/s42250-022-00328-1

ORIGINAL ARTICLE

The Fast-Efficient Adsorption Process of the Toxic Dye onto Shells Powders of Walnut and Peanut: Experiments, Equilibrium, Thermodynamic, and Regeneration Studies

Mohammed Benjelloun[1] · Youssef Miyah[1] · Rabia Bouslamti[1] · Loubna Nahali[1] · Fatiha Mejbar[1] · Sanae Lairini[1]

Received: 13 December 2021 / Accepted: 29 January 2022 / Published online: 9 February 2022

Abstract
The toxicity of the textile industry's discharges is a major concern for all authorities around the world as it negatively affects water quality and human health. In this regard, this study aims to prepare two innovative materials based on walnut shells (WS) and peanut shells (PS) as two promising, low-cost, and environmentally friendly bio-adsorbents to remove the toxic dye methylene blue (MB) in an aqueous solution. The surface morphological and functional properties of WS and PS materials were characterized by FTIR, SEM-EDX, and pHpzc to predict the likely adsorption mechanism. The performance of the adsorption method and the high selectivity of the two materials leads to a remarkable competition between the MB dye and different ions from pH variation and metal salts. The optimum adsorption capacity was 101.43 mg g^{-1} and 67.42 mg g^{-1} on treated walnut shells (TWS) and treated peanut shells (TPS), respectively, for 60 mg L^{-1} as the initial concentration of MB, particle size = 90 µm, pH 6 at a temperature of 20 °C and 0.5 g L^{-1} of the adsorbent. The adsorption experimental data followed Langmuir's isotherm and Pseudo-second-order's kinetic model. The thermodynamic parameters of MB adsorption on TWS and TPS show that the process is physical, endothermic, and spontaneous. In addition to the regeneration capacity, the overall cost of the adsorption process for one liter of methylene blue dye was $0.6968 with walnut shells and $0.6965 with peanut shells, showing the technology's economic viability and eco-industrial potential. In addition, the reuse of inexpensive adsorbents explains the importance of economic, environmental, and regenerative aspects of biomaterials.

Keywords Adsorption · Isotherm · Kinetic · Regeneration · Selectivity · Thermodynamic

1 Introduction

In recent decades, several researchers have reported that the textile industry uses very large quantities of dyes and subsequently produces discharges that are too loaded with colored pollutants [1–3]. Pollution of water by textile effluents laden with contaminants is a serious problem facing not only the environment but also human health. From a human health perspective, external exposure to methylene blue (MB) can cause skin irritation and permanent eye damage, inhaling it may cause rapid or difficult breathing and increased heart rate and its ingestion can irritate the gastrointestinal tract, nausea, loss of sweat, mental confusion, cyanosis and necrosis of human tissue [4, 5]. From an environmental standpoint, the discharge of these toxic pollutants into the water reduces the diffusion of light necessary to maintain the stability of aquatic life [6]. For this reason, several physicochemical processes have been used to treat colored effluents, such as coagulation-flocculation, oxidation, filtration, and adsorption [7–11]. Although these processes reduce wastewater pollution factors, they remain limited by their exorbitant costs and incomplete contaminants removal [12]. Adsorption is one of the most effective methods due to its high performance, flexibility, its simplicity of design, low energy demand, selectivity, and its important use for the treatment of water contaminated by textile dyes because this method is considered environmentally friendly and does not leave any pollutant molecular fragment [13–17]. The latter has been the subject of several studies: Koyuncu and Kul asserts that the active charcoal of non-living lichen *Pseudevernia furfuracea* was efficient to

✉ Mohammed Benjelloun
Mohammed.benjelloun94@gmail.com

[1] Laboratory of Materials, Processes, Catalysis, and Environment, School of Technology, Sidi Mohamed Ben Abdellah University, Fez, Morocco

adsorb the methylene blue [18], Öztürk et al. found that the bacteria *Rhodopseudomonas palustris* 51ATA was a promising adsorbent for Fast Black K azo dye [19], Tukaram bai et al. reported that the cane bagasse was performent to adsorb eosin yellow [20]. In addition to these studies, other scientific works could be mentioned as Arab et al. who observed the effective behavior of zinc oxide and curcumin nanoparticles were to adsorb Congo red [21], Siraorarnroj et al. who noticed that mulberry (*Morus alba* L.) leaf residue was a promising adsorbent for methyl orange [22], and Karaman et al. who found that orange peel waste was effective to adsorb Congo red [23]. Many researchers have studied the methylene blue adsorption on different materials such as Phosphoric Acid-Treated Balanites *Aegyptiaca* Seed Husks Powder [24], mango leaf powders [25], and *Caesalpinia ferrea* [26]. Biological treatment corresponds to a transfer of organic matter with the production of mud explains the performance of biomass for the degradation of textile effluents having a very high concentration of organic matter [27]. Besides, some scientific researchers have demonstrated the magnificence of the adsorbent properties of peanut and walnut shells on various synthetic dyes: For peanut shells, Garg et al. studied the adsorption property of activated carbon in peanut shells to remove acid yellow 36 [28]. Garg et al. studied the adsorption property of activated carbon in encapsulated alginate peanut shells to remove the Direct Blue-86 dye [29]. Liu et al. investigated the biosorption of crystal violet on the residue of fermented peanut shells [30]. For the walnut shells, Hajialigol and Masoum studied the performance of the nano-biomass based on the chemical activation of nutshells in the elimination of malachite green [31], as for Pang et al. have shown that pecan-based biomass could be a competitive adsorbent in terms of a possible real application to remove the crystal violet dye [32]. The novelty and originality of our scientific work are integrated into a process of valorization of walnut shells and peanut shells as food wastes abundantly available in municipal landfills by exploiting them in an innovative experimental project based on the preparation of effective adsorbents to be used for the removal of the methylene blue dye (MB) present in textile waters with consideration of the profitability and cost-effectiveness ratio. Various parameters were studied, such as the contact time, the initial concentration of dye, the adsorbents dose, the pH, the temperature of the solution, the adsorbents particle size, and the ionic strength. The kinetic adsorption data were tested by pseudo-first-order, pseudo-second-order kinetic models, and intra-particle diffusion. The equilibrium data were analyzed using the isotherms of Langmuir, Freundlich, and Dubinin Radushkevich. The effect of temperature on the adsorption of the dye was also studied and the thermodynamic parameters were determined. Then, aiming at an eco-environmental approach, several regeneration cycles were performed to avoid the transfer of pollution from liquid to solid. Finally, to evaluate the economic performance of the two adsorbents TWS and TPS, and their applicability on an industrial scale, the cost estimation of the methylene blue adsorption process was based on the analytical accounting of the prices of all the raw materials and chemicals used.

2 Materials and Methods

2.1 Adsorbate Preparation

The adsorbate used in the present study is methylene blue (MB) of purity 99% with formula $C_{16}H_{18}ClN_3S$ and molecular weight 319.852 g mol^{-1}. Several solutions of the MB dye were prepared by dilution with ultrapure water from a stock solution of concentration 1 g L^{-1}. Then, absorbances were obtained using UV–visible spectroscopy which gives us a maximum wavelength $\lambda_{max} = 664$ nm.

2.2 Adsorbents Preparation

Walnut shells and peanut shells are two natural bio-adsorbents from a local market in the city of Fez, Morocco. These biomaterials were washed with ultrapure water to remove adhering impurities, dried, then ground, and sieved to obtain different fractions. Then, 200 ml of ethanol (95%) was added to each fraction of our bio-adsorbents to solvate the different organic molecules present in the samples. After that, H_2O_2 (30%) was added as a bleaching agent to oxidize any non-solvated organic matter. Finally, the two treated bio-adsorbents were oven-dried for 24 h at 100 °C and sieved to obtain the treated walnut shells (TWS) and treated peanut shells (TPS).

2.3 Biosorption Process

Different characterization techniques were used to identify the composition of the main constituents of the treated walnut shell (TWS) and treated peanut shell (TPS) powders. Fourier transform infrared spectroscopy is an important tool to identify functional groups capable of adsorbing pollutant molecules onto TWS and TPS adsorbents. Scanning electron microscopy analyses require that the powders of treated peanut shells and treated walnut shells are granulated by a granulating machine that applies pressure to the powder. The isoelectric pH (zero charge point pH_{pzc}) of the two bio-adsorbents was determined using the method applied by several researchers [33–36]. It consists of adding 20 ml of sodium chloride (0.05 M) to several 50 ml polystyrene beakers and adjusting the pH (2–12) by adding drops of hydrochloric acid and sodium hydroxide (0.1 M). After shaking the suspensions at 25 °C for 48 h, they were filtered through a membrane filter (0.45 µm pore diameter)

before measuring the final pH values. The zero charge point value pH_{pzc} was determined by the point of intersection of the $\Delta pH = pH_{final} - pH_{initial}$ curve with the $pH_{initial}$ axis. The efficiency of the TWS and TPS biosorbents was tested for the removal of methylene blue (MB) dye. Several parameters such as contact time (0–60 min), initial methylene blue concentration (30–60 mg L^{-1}), adsorbent dose (0.5–2 g L^{-1}), particle size (90–200 µm), pH (2–12), and temperature (20–60 °C) were studied. The dye solution was withdrawn every five minutes, centrifuged, and then filtered through syringe filters (0.45 µm) and then immediately measured the absorbance of the supernatant using a UV–visible spectrophotometer with $\lambda_{max} = 664$ nm. The performance of the adsorbent is generally represented by the adsorption capacity at time t (Q_t, mg g^{-1}) which was calculated based on the difference between the initial concentration (C_i, mg L^{-1}) and the concentration at time t (C_t, mg L^{-1}) using Eq. (1) [37]:

$$Q_t = \frac{C_i - C_t}{W} V \quad (1)$$

where C_i is the initial concentration of methylene blue (mg L^{-1}), C_t is the concentration of methylene blue in the time t (mg L^{-1}), V is the volume of the solution (L), W is the weight of the adsorbent (g), and Q_t is the amount of adsorption at time t.

3 Results and Discussion

3.1 Characterization of the Adsorbents

3.1.1 Fourier Transform Infrared Spectroscopy

The spectrum in Fig. 1 obtained by Fourier transform infrared spectroscopy (FTIR) in a vague range that varies between 400 and 4000 cm^{-1} confirms the presence of the absorption bands characterizing the treated walnut shells (Fig. 1a) and the treated peanut shells (Fig. 1b).

For the treated walnut shell infrared spectrum shown in Fig. 1a: the band centered at 3329 cm^{-1} refers to the alcohol groups' O–H stretching vibration [38, 39]. The 2926 cm^{-1} and 2856 cm^{-1} bands are due to the CH stretching vibrations in the methyl group [31, 40]. The absorption bands in 1607 cm^{-1} refer to stretching vibrations of groups C=O, while the skeletal vibrations C=C lead to two other bands at approximately 1512 cm^{-1} and 1425 cm^{-1} [41, 42]. The 1738 cm^{-1} plug is derived from the C=O group of carbonyl compounds (ketones, aldehydes, carboxylic compounds, esters) [40, 43]. The bands at 1315, 1236, and 1022 cm^{-1} are due to C–O stretching vibrations in alcohols, phenols, or ether groups [31, 44]. The bands between 893 and 663 cm^{-1} correspond to aromatic bands attributed to the bending vibrations of the CH groups [45, 46].

For the infrared spectrum of treated peanut shells represented in Fig. 1b: The band located at 3319 cm^{-1} corresponds to the O–H stretching vibration of hydroxyl groups which can indicate the presence of cellulosic structure in the adsorbent surface [47, 48].The bands at 2920 cm^{-1} and 2858 cm^{-1} are attributed to the stretching vibrations of C–H in the methyl groups on the surface, which can present the lignin structure [47, 49]. The absorption bands in the

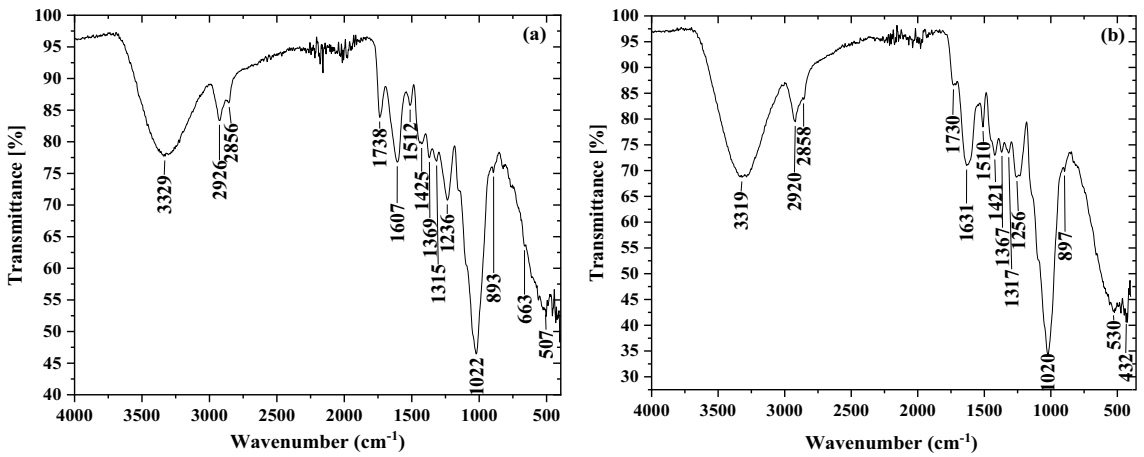

Fig. 1 The infrared spectrum of treated walnut shells (**a**) and treated peanut shells (**b**)

region of approximately 1631 cm^{-1} correspond to stretching vibrations of groups C=C aromatic rings [47, 50], while the O–H twisting vibrations and aliphatic CH_3 and CH_2 distortions in cellulose and lignin structures lead to another band to approximately 1367 cm^{-1} [51]. The plug which is of the order of 1730 cm^{-1} is derived from the group C=O extending vibrations of keto carbonyl gatherings or carboxylic groups [47]. The intense band at around 1020 cm^{-1} is attributed to the C–O of alcohol, carboxyl, or phenol [50]. The band in 530 cm^{-1} could be attributed to the in-plane ring twisting.

3.1.2 Surface morphology by SEM-EDX

Observation with a scanning electron microscope (SEM) coupled with energy-dispersive X-ray spectroscopy (EDX) shows the surface morphology of peanut shells and the walnut shells biosorbents. SEM micrographs of the TWS and TPS adsorbents are shown in Fig. 2.

The images presented in Fig. 2 highlight the fibrous and irregular structure of the TWS and TPS adsorbents. This fibrous structure explains the stiffness of the lignocellulosic material [52]. Chemical analysis by EDX shows that both bio-adsorbents are mainly formed of the elements Carbon and Oxygen. Similar EDX elemental distribution results were reported for mesopore silica composite from rice husk with activated carbon from coconut shell [53], tamarind fruit shell powder [54], banana peels, and eggshells [55]. In general, the morphological and elemental analysis of the surfaces, for each of the two biomaterials, confirms their ability to uptake toxic molecules present in an aqueous solution.

3.2 Effect of Contact Time and Initial Concentration

Figure 3 represents the evolution of the adsorbed quantity of methylene blue per gram of treated walnut shells and treated peanut shells as a function of the contact time at different initial dye concentrations (from 30 to 60 mg L^{-1}) with a constant mass of adsorbent of 0.5 g L^{-1}, at T = 20 °C and for 60 min.

The adsorption kinetics of methylene blue on both the treated walnut shells (Fig. 3a) and the treated peanut shells (Fig. 3b) show paces characterized by rapid adsorption from the first minutes of contact, followed by a slow increase until

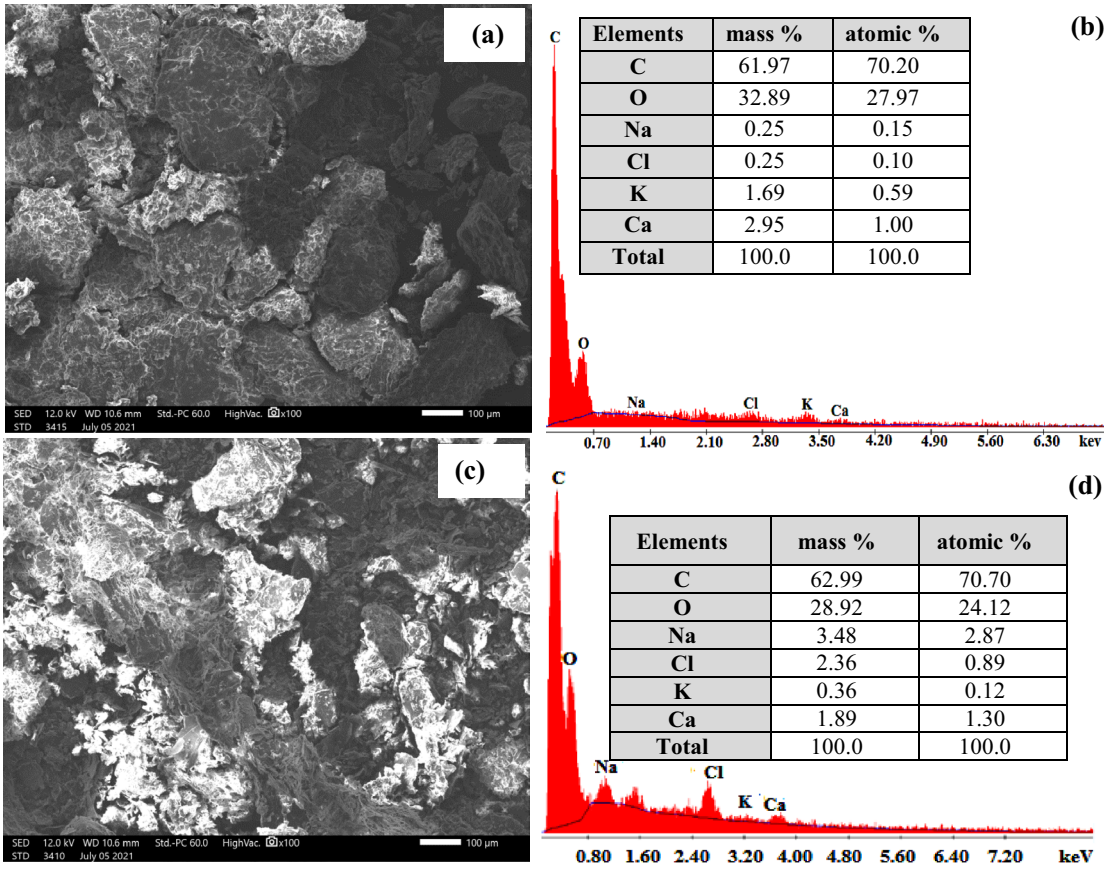

Elements	mass %	atomic %
C	61.97	70.20
O	32.89	27.97
Na	0.25	0.15
Cl	0.25	0.10
K	1.69	0.59
Ca	2.95	1.00
Total	100.0	100.0

Elements	mass %	atomic %
C	62.99	70.70
O	28.92	24.12
Na	3.48	2.87
Cl	2.36	0.89
K	0.36	0.12
Ca	1.89	1.30
Total	100.0	100.0

Fig. 2 SEM-EDX of TWS (**a**, **b**) and TPS (**c**, **d**)

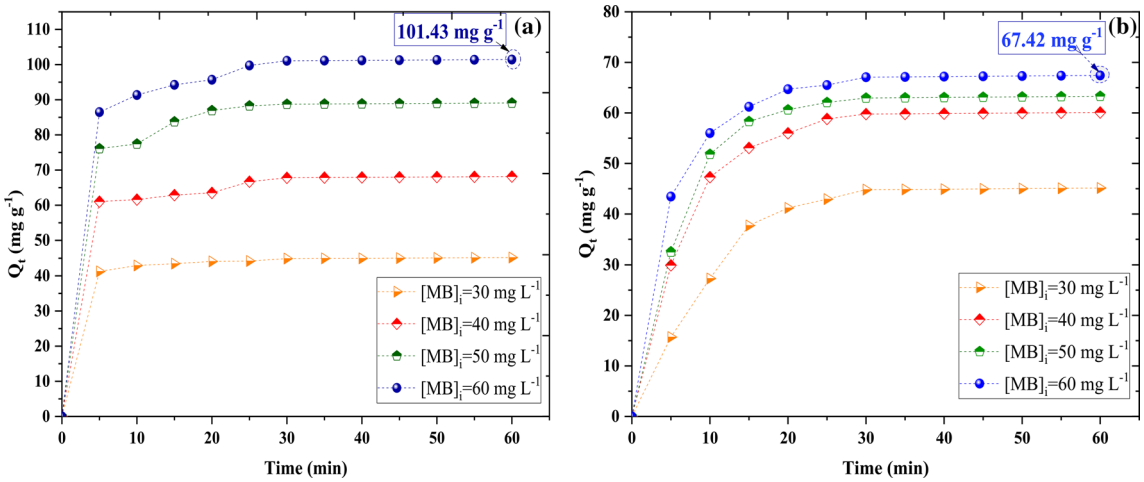

Fig. 3 Effect of methylene blue dye initial concentration on adsorption capacity onto treated walnut shells (**a**) and treated peanut shells (**b**) (T = 20 ° C, adsorbent dose = 0.5 g L^{-1}, particle size = 90 µm)

reaching a state of equilibrium at t = 30 min. This could be explained by the fact that the sorption sites are open at the beginning and that the molecules of methylene blue easily access these sites. Beyond t = 30 min, the adsorption capacities remain constant because of the binding site saturation and increase with the increase in the initial concentration of methylene blue. This increase can be attributed to the presence of an inordinate range of molecules that can be uptaken on the sites on the surface of the adsorbent [56, 57], and/or to the fact that the molecules of the dye can occupy more sorption sites at higher initial concentrations [16, 28], and/or to the fact that the driving force, necessary to overcome all the mass transfer resistances of the dye molecules between the solution and the surface, is provided by the high value of the concentration gradient [58, 59]. Furthermore, according to Fig. 3, the optimal initial concentration of methylene blue dye is 60 mg L^{-1} with 101.43 mg g^{-1} and 67.42 mg g^{-1} as adsorption capacities on treated walnut shells and treated peanut shells respectively.

3.3 Effect of the Adsorbent Amount

This study was carried out to assess the adsorption capacity of methylene blue by different doses of TWS and TPS from 0.5 to 2 g L^{-1} by keeping constant the initial concentration of methylene blue at 60 mg L^{-1} and the temperature of the solution at 20 °C (Fig. 4).

The adsorbed amounts of MB on TWS are 99.98 mg g^{-1}, 46.66 mg g^{-1}, 26.03 mg g^{-1}, and 12.44 mg g^{-1} and on TPS are 60.47 mg g^{-1}, 28.58 mg g^{-1}, 16.47 mg g^{-1} and 10.09 mg

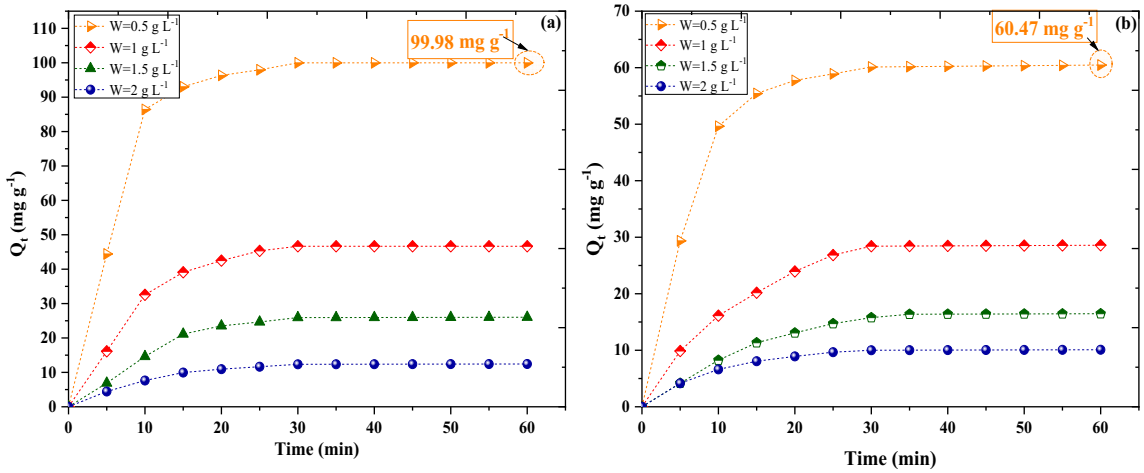

Fig. 4 Effect of the treated walnut shells (**a**) and treated peanut shells (**b**) amounts on methylene blue adsorption capacity (T = 20 °C, [MB] = 60 mg L^{-1}, particle size = 90 µm)

g^{-1} for adsorbent doses 0.5 g L^{-1}, 1 g L^{-1}, 1.5 g L^{-1}, and 2 g L^{-1}, respectively. These results show that the adsorption capacity of methylene blue decreases by increasing the adsorbent's dose. This can be explained by the saturation of most adsorption sites with high doses of adsorbent [60, 61].

3.4 Effect of Particle Size

Particle size is a key parameter for the study of MB dye adsorption on the surface of TWS and TPS. To this end, the study of adsorbent particle size allows the determination of the optimal particle size through a series of experiments conducted with different particle sizes from 90 to 200 µm using 60 mg L^{-1} of methylene blue, 0.5 g L^{-1} of adsorbent, pH 6, at room temperature and under stirring at 250 rpm (Fig. 5).

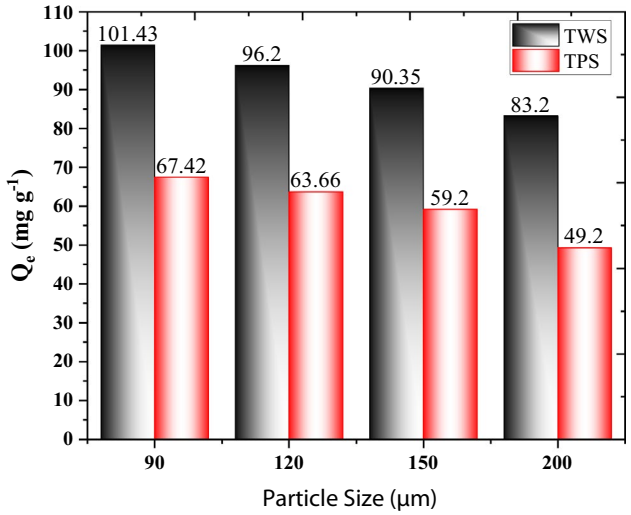

Fig. 5 Effect of treated walnut shell and treated peanut shell particles size on methylene blue dye adsorption (T = 20 °C, [MB] = 60 mg L^{-1}, adsorbent amount = 0.5 g L^{-1})

According to Fig. 5, the adsorption capacity of the methylene blue dye decreases by increasing the particle size of each of the two bio-adsorbents. The adsorption equilibrium capacity for walnut shells goes from 101.43 mg g^{-1} at 90 µm to 83.2 mg g^{-1} at 200 µm. The same thing is observed in the case of peanut shells when the adsorption equilibrium capacity decreases from 67.42 mg g^{-1} at 90 µm to 49.2 mg g^{-1} at 200 µm. This could be due to the availability of more active sites and larger specific surface area for the bio-adsorption process in fine particle sizes more than in bigger ones [62, 63]. In all the batch adsorption experiments, a particle size of 90 µm was picked to be the best size.

3.5 Effect of the Initial pH Solution

The study of the acid–base behavior of the treated walnut shells and treated peanut shells surfaces' in the presence of the methylene blue dye makes it possible to predict a probable selectivity and mechanism of the liquid phase adsorption on the surface of the solid phase [64]. So it is wise to know the adsorption efficiency at different pH. In this case, 0.5 g L^{-1} of the adsorbent is introduced into a solution of the dye having an initial concentration of 60 mg L^{-1} at T = 20 °C. The solutions of sodium hydroxide and hydrochloric acid (0.1 N) were used to adjust the pH of the test solutions which were made with a pH range of 2–12 (Fig. 6).

Figure 6a shows that the adsorption capacity increases by increasing the pH. Indeed, the weak elimination of the cationic dye, methylene blue, in an acid medium can be explained by the competition between protons and cations formed by methylene blue [65]. According to Fig. 6b, the

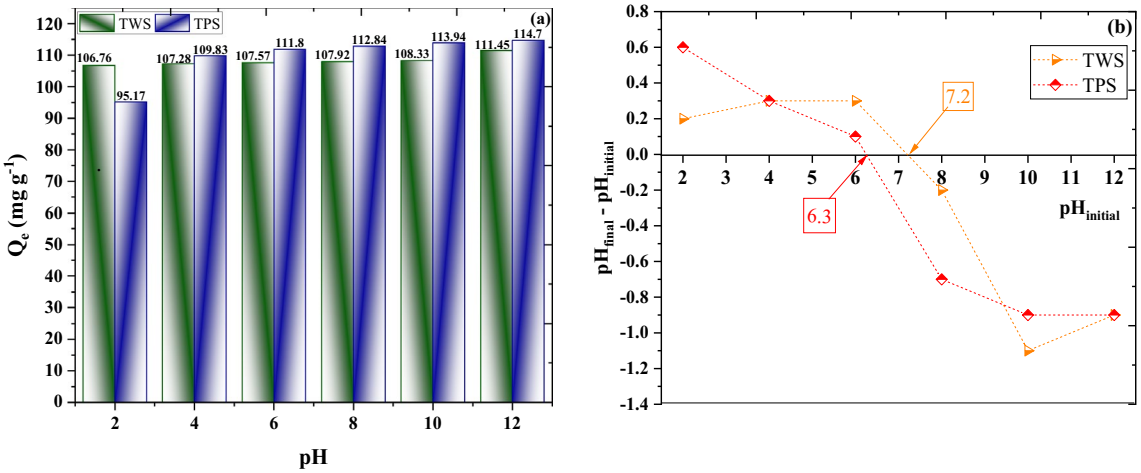

Fig. 6 pH solution effect on methylene blue adsorption capacity onto TWS and TPS (T = 20 °C, [MB] = 60 mg L^{-1}) (**a**), Amount of adsorbent = 0.5 g L^{-1}, particle size = 90 µm), pH_{pzc} of TWS and TPS (**b**)

two pH_{pzc} values of treated walnut shells and treated peanut shells obtained are equal to 7.2 and 6.3, respectively. As the pH is increased, there is a decrease in the hydrogen cations, so the adsorbents' charge becomes negative, which promotes the adsorption of the methylene blue cations by the electrostatic attraction phenomenon [66, 67].

3.6 Effect of the Temperature

The temperature of the solution is another characteristic of great interest in kinetic adsorption processes since its influence on the diffusion process is very important, especially for textile effluents which are released with considerable heat due to dyeing, bleaching, and washing procedures [30]. For this reason, we have introduced the adsorbent (0.5 g L^{-1}) into methylene blue solutions at an initial concentration (60 mg L^{-1}) with a temperature range (20–60 °C), and the results were obtained are shown in Fig. 7.

From Fig. 7, it can be noted that when the temperature increases, the adsorption rate also increases. The increase of the adsorption capacity as a function of time could be probably explained by the increase in the active sites on the adsorbent surface [68] and/or the decrease in the mass transfer resistance of adsorbate in the boundary layer [69], and/or the endothermicity of the reaction [16, 59, 70], and/or the increase of chemical adsorbate–adsorbent interaction [16], and/or intraparticle diffusion in the pores of the adsorbent with the increased speed at a higher temperature [68], and/or modification of the internal structure of the adsorbent [29]. In the present study, the system shows that the adsorption capacities of methylene blue on treated walnut shells (Fig. 7a) and treated peanut shells (Fig. 7b) increase with temperature. It can be observed that when the temperature increases from 20 to 60 °C, the adsorption capacity on treated walnut shells increases from 86.51 to 93.55 mg g^{-1} and from 60.47 to 103.15 mg g^{-1} for treated peanut shells. Consequently, the adsorption process is endothermic and requires less energy because, when the system is exothermic, it favors low temperatures for improved adsorption [71].

3.7 Effect of Ionic Strength

The presence of alkali metals (such as sodium and potassium), alkaline-earth metals (such as barium, calcium, and magnesium), and transition metals (such as cuprous ions, chromium (III)) in textile wastewater causes interionic interactions of all ions, such as molecular attractions or repulsions that could influence the adsorption phenomenon. To research the effect of ionic strength on the adsorption phenomenon of methylene blue on treated walnut shells and treated peanut shell powders, various concentrations of barium chloride, calcium chloride, and sodium chloride (0.1–0.5 M) was added at the initial concentration of 60 mg L^{-1} of methylene blue and adsorbent mass (0.5 g L^{-1}).

The effect of sodium chloride, barium chloride, and calcium chloride salts on the adsorption quantity of Methylene Blue dye on treated walnut shells and treated peanut shells is seen in Fig. 8. The results show that there is a decrease in equilibrium adsorption capacity for the two bio-adsorbents when there is a growth of each salt concentration, especially for divalent metallic ions (Ba^{2+} and Ca^{2+}) because they are more competitive than Na^{+} (monovalent) against the methylene blue cationic dye: For the treated walnut shells, increasing the concentrations of salts from 0 to 0.5 M decreases the adsorption capacity from 101.43 to 94.1 mg g^{-1} in sodium chloride, to 81.2 mg g^{-1} in barium chloride and 80.1 mg g^{-1} in calcium chloride. In the case of the treated peanut shells, increasing the salt concentrations from 0 to 0.5 M

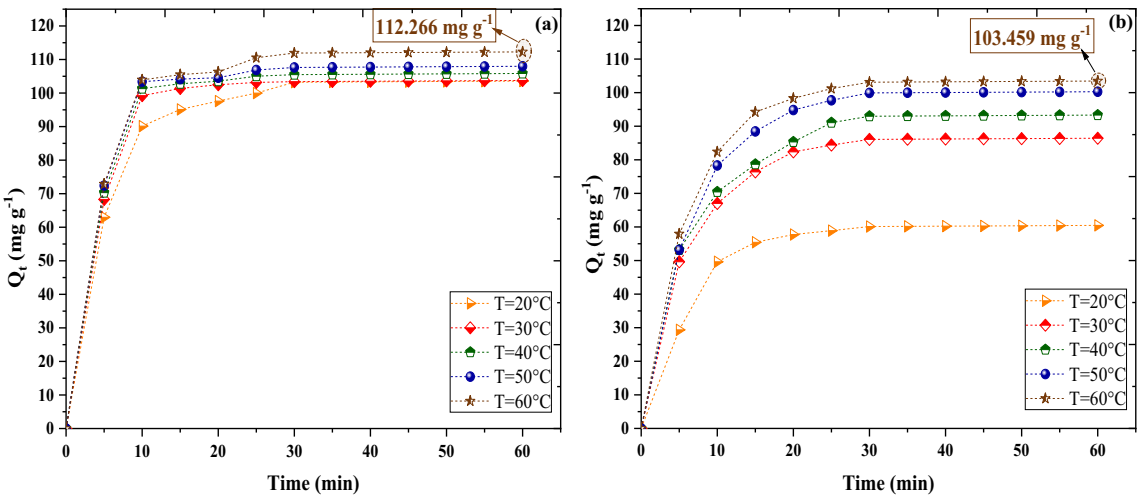

Fig. 7 Effect the solution temperature on methylene blue adsorption capacity onto TWS (**a**) and TPS (**b**) ([MB] = 60 mg L^{-1}, Amount of adsorbent = 0.5 g L^{-1}, particle size = 90 µm)

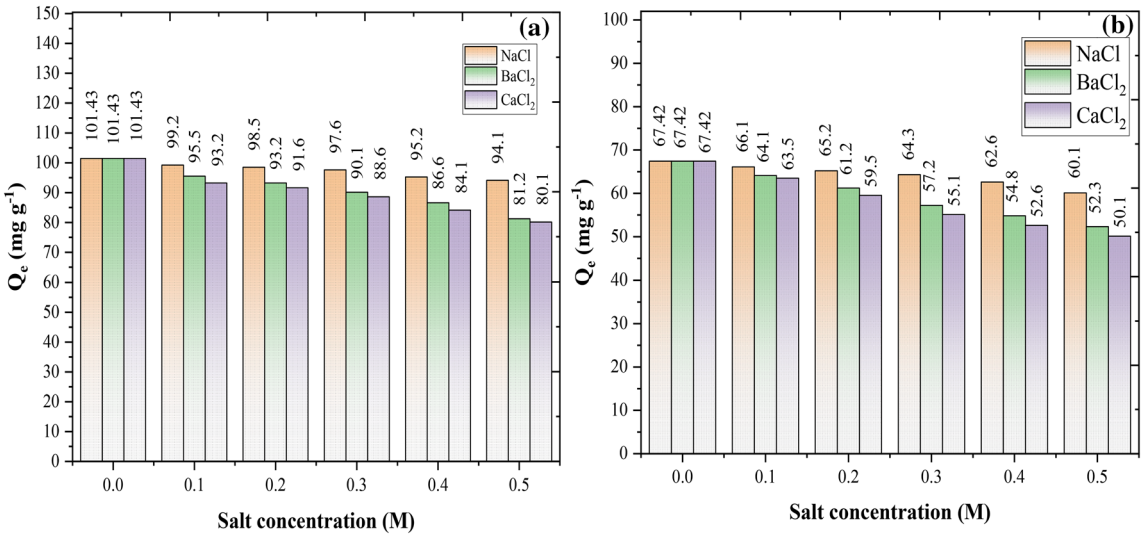

Fig. 8 Effect of ionic strength on Methylene blue adsorption on treated walnut shells (**a**) and treated peanut shells (**b**) ([MB] = 60 mg L^{-1}, Amount of adsorbent = 0.5 g L^{-1}, particle size = 90 µm)

decreases the adsorption capacity from 67.42 to 60.1 mg g^{-1} in sodium chloride, to 52.3 mg g^{-1} in barium chloride, and 50.1 mg g^{-1} in calcium chloride. The explanation for these results could be the fact that the salt ions interfere with the molecules of the cationic dye on the surface of each of the two bio-adsorbents thus leading to the breakdown of the electrostatic interaction between the dye molecules and the adsorbent surface [10, 72–75].

3.8 Thermodynamic Studies

Thermodynamic studies are very important because they allow us to predict the behavior of the adsorbent, the appropriate temperature range for adsorption, and the nature of the sorbent and the adsorbate at equilibrium [76]. For the phenomenological description of the adsorption, and more specifically the thermodynamic behavior of the system, adsorption tests have been carried out in temperatures (293–333 K) and allow to measure the parameters which must be taken into account: ΔH° (standard enthalpy), ΔS° (standard entropy) and ΔG° (standard Free energy).

The values of ΔH° and ΔS° were obtained using the Vant-Hoff Eq. (2) [20, 77] :

$$\mathrm{Ln}\left(\mathrm{K}_e\right) = \frac{\Delta S^\circ}{R} - \frac{\Delta H^\circ}{RT} \tag{2}$$

where ΔH° is standard enthalpy, ΔS° is standard entropy, ΔG° is standard Free energy, R is the perfect gas constant (R = 8.314 J mol^{-1} K^{-1}), T is the absolute temperature of the solution, and K_e is the partition coefficient at equilibrium calculated by using Eq. (3):

$$K_e = \frac{Q_e}{C_e} \tag{3}$$

where Q_e is Adsorption capacity at equilibrium, and C_e is Concentration of adsorbate at equilibrium.

The values of ΔH° and ΔS° were calculated respectively from the slope and the ordinate at the origin of Ln (K_e) as a function of 1/T as represented in Fig. 9.

Values of ΔG° can be obtained from the values of ΔH° and ΔS° and the Gibbs–Helmholtz Eq. (4).

$$\Delta G^\circ = \Delta H^\circ - T\Delta S^\circ \tag{4}$$

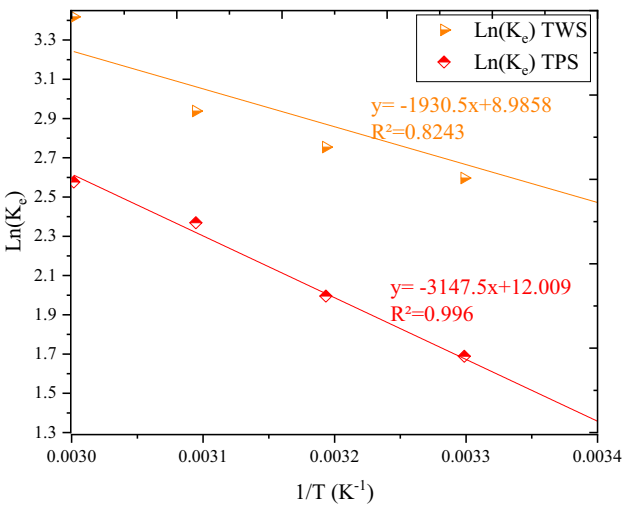

Fig. 9 Graphical representation of Ln (K_e) as a function of the inverse of the temperature (1/T)

Table 1 Thermodynamic parameters for the adsorption of methylene blue onto treated walnut shells and treated peanut shells

Thermodynamic parameters	Temperature (K)	Values for TWS	Values for TPS
ΔG° (kJ mol^{-1})	293	− 6.1779	− 3.0671
	303	− 6.4197	− 4.1303
	313	− 7.041	− 5.0649
	323	− 7.7606	− 6.2309
	333	− 9.3303	− 6.9983
ΔH° (kJ mol^{-1})	–	16.0511	26.1698
ΔS° (kJ mol^{-1})	–	0.0747	0.0998

where ΔH° is standard enthalpy, ΔS° is standard entropy, ΔG° is standard free energy, and T is the absolute temperature of the solution. Table 1 represents the values of ΔH°, ΔS°, and ΔG°.

Positive values of ΔH° show that the adsorption process is endothermic. Besides, |ΔH°| <60 kJ mol^{-1} shows that the adsorption process is based on physical interactions (physisorption) [70]. The positive values of ΔS° for the adsorption of methylene blue on walnut shells and peanut shells indicate that the randomness of the polluting molecules increases at the interface of the adsorbent-adsorbate solution [78, 79]. ΔG° < 0 kJ mol^{-1} indicates that the adsorption of methylene blue on both walnut shells and peanut shells is feasible and spontaneous [80, 81].

3.9 Adsorption Isotherms

In the analysis of adsorption processes, the equilibrium data are normally expressed in adsorption isotherms: isotherms are an essential part of the modeling of adsorption and therefore of the design, calculation of yields, and costs of adsorption. The adsorption isotherms allow us to estimate the degree of purification that can be achieved, the quantity of adsorbent required, and the sensitivity of the process to the concentration of the product [82].

3.9.1 Langmuir's Isotherm

Langmuir's (1918) model, based on thermodynamic and kinetic considerations, is based on the existence of free sites on the surface of the adsorbent material where the adsorption of the solute takes place. The use of this model implies reversible adsorption supposedly monolayer. This theory also admits that the adsorption energy is uniform on the surface of the adsorbent [83]. The mathematical expression of the Langmuir isotherm is given by Eq. (5) [84] :

$$Q_e = \frac{Q_L k_L C_e}{1 + k_L C_e} \tag{5}$$

The linear representation of the Langmuir model can be represented by Eq. (6) [70] :

$$\frac{C_e}{Q_e} = \frac{1}{k_L Q_L} + \frac{C_e}{Q_L} \tag{6}$$

where C_e is Concentration at equilibrium (mg L^{-1}) of methylene blue; Q_e is Adsorption capacity of methylene blue at equilibrium (mg g^{-1}); Q_L (mg g^{-1}) and k_L (L mg^{-1}) are Langmuir constants relating to the adsorption capacity and the adsorption energy that are obtained by determining the slope and the ordinate at the origin of the C_e/Q_e versus C_e. The results are listed in Table 2.

The dimensionless constant separation factor R_L is used to express the essential characteristics of the Langmuir isotherm, which is given by Eq. (7) [70]:

$$R_L = \frac{1}{1 + k_L C_i} \tag{7}$$

where K_L (L mg^{-1}) is Langmuir constant, C_i (mg L^{-1}) is the initial concentration in the liquid phase, and R_L is the dimensionless parameter of equilibrium intensity or adsorption intensity. Its value indicates the model of isothermal adsorption characteristics as follows [85]: If $R_L = 0$, the adsorption is invertible. If $0 < R_L < 1$, the adsorption is favorable. If $R_L = 1$, the adsorption is linear. If $R_L > 1$, adsorption is unfavorable.

For the adsorption of methylene blue on walnut shells and peanut shells, the R_L values listed in Table 2 are 0.067 and 0.037 respectively, which indicates that adsorption on both the two adsorbents is a favorable process.

Table 2 Isotherm constants for methylene blue adsorption onto walnut shells and peanut shells

Isotherm model	Model parameters	Values for walnut shells	Values for peanut shells
Langmuir	Q_L (mg g^{-1})	19.0114	72.9927
	k_L (L mg^{-1})	0.2334	0.4322
	R_L^2	0.9999	0.9979
	R_L	0.067	0.037
	S_a (m^2 g^{-1})	70.5620	270.9171
Freundlich	k_F ($mg^{1-1/n}$ g^{-1} $L^{1/n}$)	3289.859	45.9429
	n_F	0.4653	8.7108
	R_F^2	0.9803	0.9583
Dubinin Radushkevich	E (kJ mol^{-1})	0.2357	0.5000
	q_{DR} (mg/g)	18.4248	67.2556
	K_{DR} (mol^2 kJ^{-2})	9.000	2.000
	R_{DR}^2	0.9922	0.8428

The specific surface of an adsorbent could be estimated by the Langmuir isotherm through the following Eq. (8) [86, 87] :

$$S_a = \frac{Q_L N_A S_{MB}}{M_{MB}} (8) \quad (8)$$

where M_{MB} is the molecular mass of methylene blue dye (mg mol^{-1}) and it is equal to 319,850 mg mol^{-1}, N_A is Avogadro's number (6.02×10^{23} mol^{-1}), S_a is the adsorbent surface ($m^2 g^{-1}$); S_{MB} is the contact area for each molecule of methylene blue dye (m^2) and is equivalent to 1.972×10^{-18} m^2.

The values of the specific surface of each of the two adsorbents are also noted in Table 2.

3.9.2 Freundlich's Isotherm

Freundlich considers that there are different types of adsorption sites for a different energy, but with the same entropy, distributed according to an exponential law as a function of the heat of adsorption. The site density decreases exponentially and the quantity adsorbed at equilibrium is written as the following Eq. (9) [65, 88] :

$$Q_e = k_F (C_e)^{\frac{1}{n}} \quad (9)$$

The linear representation of the Freundlich model can be written as the following Eq. (10) [89] :

$$Ln(Q_e) = Ln(k_F) + \frac{1}{n} Ln(C_e) \quad (10)$$

where k_F is Freundlich's adsorption capacity and n is adsorption intensity.

For the calculation of the equilibrium constants of the Freundlich adsorption, the linear curve Ln (Q_e) versus Ln (C_e) is used. The slope (1/n) with $0 < 1/n < 1$: is a measure of the adsorption intensity or the heterogeneity of the surface and as its value approaches 0, the surface becomes more heterogeneous. k_F is obtained by the exponential of the intercept.

3.9.3 Dubinin Radushkevich Isotherm

Dubinin Radushkevich's isothermal model was developed to describe the effect of the porous structure of adsorbents [90–93]. It was based on the theory of adsorption potential and assumed that the adsorption process was related to the filling of the micropore volume as opposed to the layer-by-layer adsorption on the walls of the pores [94]. The mathematical expression of Dubinin Radushkevich isotherm is given by Eq. (11) [95] :

$$Q_e = Q_{DR} e^{-\beta \epsilon^2} \quad (11)$$

The linear representation of the Dubinin Radushkevich model can be written as the following Eq. (12) [96] :

$$Ln(Q_e) = Ln(Q_{DR}) - k_{DR} \epsilon^2 \quad (12)$$

where k_{DR} (mol^2 kJ^{-2}): Isothermal constant of Dubinin Radushkevich, Q_{DR} is Dubinin Radushkevich theoretical maximum adsorption capacity and ε is Polanyi's potential represented in the Eq. (13):

$$\epsilon = RT\, Ln\left(1 + \frac{1}{C_e}\right) \quad (13)$$

where R is the perfect gas constant (8.314 J mol^{-1} K^{-1}), T (K): absolute temperature, Q_{DR} (mg g^{-1}): maximum adsorption capacity in micropores, and Q_e (mg g^{-1}): adsorption capacity at equilibrium.

The average free energy of adsorption (kJ mol^{-1}) can be calculated as the following Eq. (14) [96] :

$$E = \sqrt{\frac{1}{2k_{DR}}} (14) \quad (14)$$

Plotting Ln (Q_e) as a function of ε^2 provides Q_{DR} and k_{DR}. Langmuir's isotherm constants do not explain the properties of the physical or chemical process. However, the average energy of adsorption (E) calculated from the Dubinin Radushkevich isotherm provides important information about these properties [97]: If $E < 8$ kJ mol^{-1}, physisorption dominates the sorption mechanism, and if $8 < E < 16$ kJ mol^{-1}, ion exchange is the dominant factor (chemisorption). In this study, the adsorption energies are 0.5 and 0.2357 kJ mol^{-1} respectively for the peanut shells and walnut shells, which suggests that the adsorption process is dominated by physical forces at all temperatures.

3.9.4 Comparison Between the Isotherms: Langmuir, Freundlich, and Dubinin Radushkevich

Based on the coefficient of determination R^2: R^2_L (0.9999) > R^2_{DR} (0.9922) > R^2_F (0.9583) for walnut shells and R^2_L (0.9979) > R^2_F (0.9583) > R^2_{DR} (0.8428) for peanut shells. Therefore, the adsorption of methylene blue onto walnut shells and peanut shells is better represented by the Langmuir model with a maximum monolayer capacity equal to 19.01 mg g^{-1} for walnut shells and 72.99 mg g^{-1} for peanut shells, which indicate that the adsorption surface is homogeneous [98–100].

3.10 Theoretical Models of Adsorption Kinetics

To model the kinetics of adsorption, three empirical models are often used: Pseudo-first-order, Pseudo-second order, and the model of intraparticle diffusion.

3.10.1 Model of the Kinetics of the Pseudo-first-order

The pseudo-first-order model, established by Lagergren, is the first speed equation describing the adsorption kinetics of an adsorbate-adsorbent couple. It is based on the quantity adsorbed. The speed of adsorption at a time t is proportional to the difference between the quantity adsorbed at equilibrium Q_e and that adsorbed at time t (Fig. 10). The equation of the pseudo-first-order is described according to the following Eq. (15) [101] :

$$\frac{dQ}{dt} = k_1\left(Q_e - Q_t\right) \tag{15}$$

where Q_e is the quantity of solute adsorbed at equilibrium (mg g^{-1}), Q_t is the quantity of solute adsorbed at time t (mg g^{-1}), and k_1 is the velocity constant of the pseudo-first-order (min^{-1}).

The integration of the Eq. 15 for the initial conditions at $Q_{t=0}$ to t=0 gives the Eq. (16) [102]:

$$Ln\left(Q_e - Q_t\right) = Ln\left(Q_e\right) - k_1 t \tag{16}$$

The quantity of solute adsorbed at equilibrium Q_e and the speed constant of the pseudo-first-order k_1 is determined from the graphic representation of $Ln(Q_e - Q_t)$ as a function of time t (Fig. 10) [103].

3.10.2 Model of the Kinetics of the Pseudo-second-order

The velocity of adsorption of the pseudo-second-order, established by Blanchard [104] also depends on the amount adsorbed at equilibrium. The kinetic equation of the pseudo-second-order is given by the following Eq. (17) [105]:

$$\frac{dQ}{dt} = k_2\left(Q_e - Q_t\right)^2 \tag{17}$$

where Q_e is the amount of solute adsorbed at equilibrium (mg g^{-1}), Q_t is The quantity of solute adsorbed at time t (mg g^{-1}), and k_2 is the velocity constant of pseudo-second-order (g mg^{-1} min^{-1}).

The integration of the last equation with the boundary conditions $Q_{t=0}$ to t = 0 takes the linear form as described by the following Eq. (18) [102] :

$$\frac{t}{Q_t} = \frac{1}{K_2 Q_e^2} + \frac{1}{Q_e}t \tag{18}$$

Plotting $1/Q_t$ as a function of time gives you a curve with a slope of $1/Q_e$ and an ordinate at the origin of $(1/(k_2 Q_e^2))$ (Fig. 11).

3.10.3 Model of the Kinetics of Intraparticle Diffusion

The kinetic model of intra-particle diffusion designed by Weber and Morris is, as its name suggests, a kinetic model based on the diffusion of the adsorbate until it enters the adsorbent [106]. The empirical equation of the model in Eq. (19) [70] :

$$Q_t = k_{ID}\sqrt{t} + I \tag{19}$$

where Q_t is the adsorption capacity at time t (mg g^{-1}), k_{ID} is the constant of the intra-particle diffusion model (mg g^{-1} $min^{-1/2}$), t is contact time (min), and I (mg g^{-1}) is boundary layer thickness.

According to Weber and Morris, if intra-particle diffusion is the limiting step in the adsorbate elimination process, the graph Qt vs. $\sqrt{t}$ should give a straight line that passes through the origin of the contact information [70, 106–108].

Referring to Fig. 12, for all initial concentrations, the first step was completed within the first eight minutes and the second step of controlling intra-particulate diffusion was reached. The third step occurred for all initial

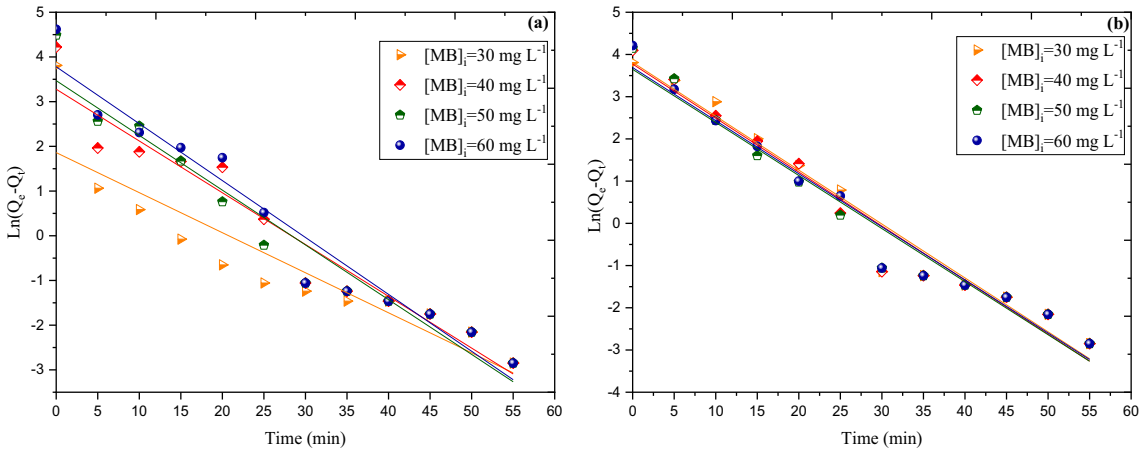

Fig. 10 Pseudo-first-order kinetic model of adsorption of methylene blue on treated walnut shells (**a**) and treated peanut shells (**b**)

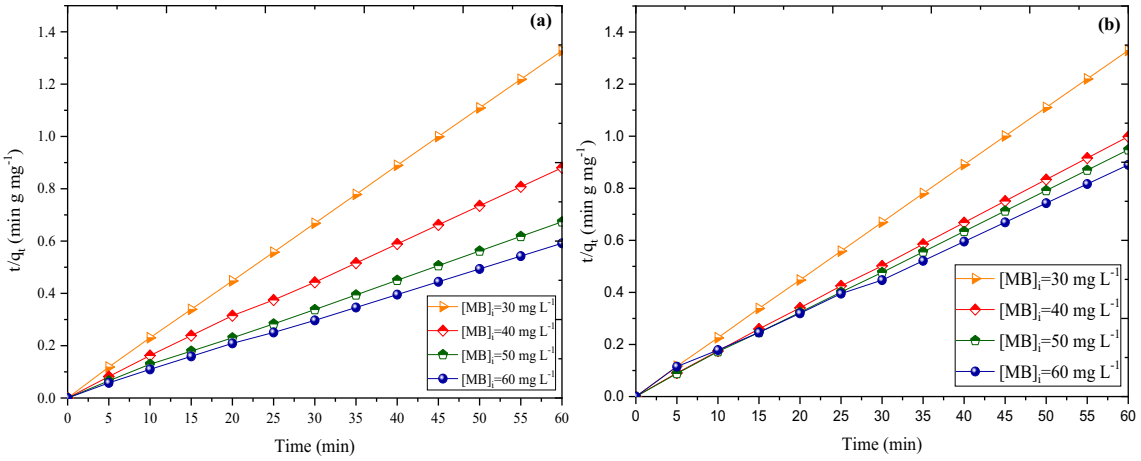

Fig. 11 Pseudo-second-order kinetic model of adsorption of methylene blue on treated walnut shells (**a**) and treated peanut shells (**b**)

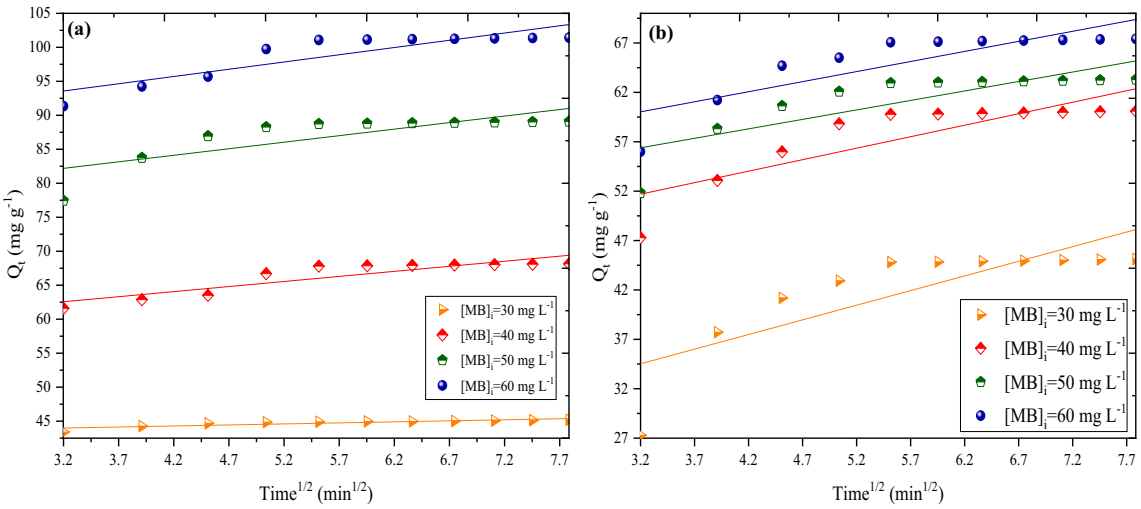

Fig. 12 Intraparticle diffusion kinetic model of adsorption of methylene blue on treated walnut shells (**a**) and treated peanut shells (**b**)

concentrations of methylene blue at 30 min. The different adsorption rates observed indicate that the adsorption rate is initially faster and then slows down as the weather increases. As can be seen in Fig. 12, the linear lines have not passed through the origin and this deviation from the origin or near the saturation may be due to the difference in transfer speed of mass between the initial and final stages of adsorption [109]. It turns out that intra-particle diffusion was not the only mechanism limiting the start of the adsorption process. The values of K_{ID}, I, and the coefficient of determination R^2 obtained for the plots are given in Table 3.

From Table 3: $R^2_2 > R^2_1 > R^2_{ID}$, therefore the most suitable model for describing the adsorption kinetics of methylene blue on both treated walnut shells and treated peanut shells is the pseudo-second-order model.

3.11 Comparison of adsorption results with other available adsorbents

The adsorption capacities of treated walnut shells and treated peanut shells were compared with other adsorbents (Table 4). These data demonstrated that walnut shells and peanut shells are effective low-cost adsorbents for removing the methylene blue dye from the aqueous phase compared to other adsorbents.

3.12 Thermal Regeneration of Adsorbents

Thermal regeneration not only removes all organic pollutants retained by physical adsorption as well as inorganic compounds from the pores of adsorbent materials without destroying their textural structure, but it also remains an

Table 3 Comparison between the Pseudo-first-order, Pseudo-second-order, and Intraparticle diffusion model adsorption rate constants, calculated and experimental q_e values for different initial methylene blue concentrations

Kinetic model	Model parameters	Methylene blue initial concentration (mg L^{-1})							
		Values for walnut shells				Values for peanut shell			
		30	40	50	60	30	40	50	60
Pseudo first order	$(q_e)_{cal}$(mg g^{-1})	6.427	26.528	32.140	43.829	45.359	43.515	38.382	40.033
	k_1(min^{-1})	0.090	0.116	0.122	0.127	0.128	0.128	0.126	0.126
	R_1^2	0.824	0.941	0.946	0.951	0.964	0.963	0.963	0.967
Pseudo second order	$(q_e)_{cal}$(mg g^{-1})	45.249	68.965	90.090	103.093	45.249	60.606	63.694	69.930
	k_2(g mg^{-1} min^{-1})	0.076	0.017	0.014	0.011	0.104	0.036	0.028	0.008
	R_2^2	1	0.999	0.999	0.999	1	0.999	0.999	0.999
Intraparticle diffusion	$(q_e)_{exp}$(mg g^{-1})	45.198	68.152	89.079	101.432	45.140	60.099	63.297	67.422
	k_{ID}(mg g^{-1} $min^{-1/2}$)	0.304	1.491	1.923	2.131	2.965	2.326	1.917	2.039
	I(mg g^{-1})	43.025	57.854	76.114	86.839	25.152	44.344	50.33	53.581
	R_{ID}^2	0.758	0.807	0.639	0.789	0.658	0.714	0.665	0.712

Table 4 Comparison of the methylene blue adsorption capacities on various adsorbents

Adsorbent	Q_e(mg g^{-1})	Contact time (min)	Isotherm	Kinetic	Process	Thermodynamic	References
Treated Walnut Shells	101.43	30	Langmuir	Pseudo Second Order	Physisorption	Endothermic Spontaneous Feasible	This Work
Treated Peanut Shells	67.42	30	Langmuir	Pseudo Second Order	Physisorption	Endothermic Spontaneous Feasible	This Work
Nitraria retusa leaves	813	–	Langmuir	Pseudo Second Order	Chemisorption	Endothermic Unspontaneous	[110]
Magnetite Nanoparticles loaded Figleaves	61.72	35	Langmuir	Pseudo Second Order	Chemisorption	–	[111]
Oued Sebou Natural Sediments	19.70	60	Freundlich	Pseudo Second Order	–	Endothermic	[112]
Untreated Husk of *Lathyrus sativus*	98.33	105	Langmuir and Temkin	Pseudo Second Order	Physisorption	Exothermic Spontaneous	[113]
Peanut shell-sulfuric acid reflux	1250	30	Langmuir	–	–	Endothermic	[114]
Sulfuric acid-treated coconut shell	50.6	60	Freundlich	Pseudo Second Order	Chemisorption	–	[115]
Waste Activated Carbon from Domestic Water Filter	15.38	60	Langmuir	Pseudo-Second-Order	Physisorption	Exothermic, Spontaneous, Favorable.	[116]
Base treated mucuna beans	19.93	40	–	Pseudo Second Order	–	Exothermic Spontaneous Feasible	[117]
Acid Washed Black Cumin Seed	73.529	30	Langmuir + Freundlich	Pseudo Second Order	–	Favorable Spontaneous Endothermic	[118]
Cinnamomum camphora leave	741	240	Langmuir	Pseudo Second Order	–	–	[119]

ecological option preventing the formation of toxic substances from the waste solid. This study highlights the overall cost of the treatment process, the importance of the reuse of low-cost materials (such as agrifood waste), and their regenerative capacity at a temperature equal to 500 °C for two hours after adsorption of methylene blue (60 mg L^{-1}) for which we obtained other adsorption capacities represented in the Fig. 13 bar graph under the same operating conditions mentioned above.

The recycled output of both treated walnut shells and treated peanut shells for the removal of methylene blue for four cycles is shown in Fig. 13. The findings revealed that the dye removal potential for treated walnut shells increased significantly from 101.43 mg g^{-1} during the adsorption to 109.55 mg g^{-1} during the first thermal regeneration cycle and then decreased to 96.2 mg g^{-1} during the second thermal regeneration cycle and then decreased to 90.5 mg g^{-1} during the third thermal regeneration cycle and then decreased to 86.5 mg g^{-1} during the fourth regeneration cycle. The same thing occurred with the peanut shells, as the dye removal potential rose from 67.42 mg g^{-1} during the adsorption to 73.5 mg g^{-1} during the first thermal regeneration cycle and then decreased to 62.2 mg g^{-1} during the second thermal regeneration cycle, and then decreased to 58.5 mg g^{-1} during the third thermal regeneration cycle, and then decreased to 51.9 mg g^{-1} during the fourth thermal regeneration cycle. This may be attributed to the fact that fresh and free pores were generated for the first thermal regeneration cycle and then a greater basic surface which promotes the dye uptakes [120]. For the other thermal regeneration cycles, there is perhaps a biomaterials deterioration caused by heat treatment [121].

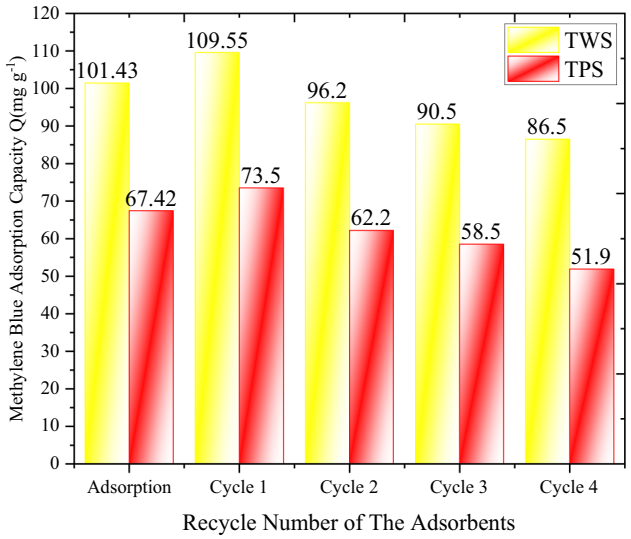

Fig. 13 Effect of thermal regeneration cycles of treated walnut shell powders and treated peanut shell powders on the adsorption capacity of methylene blue dye ([MB] = 60 mg L^{-1}, Amount of adsorbent = 0.5 g L^{-1}, particle size = 90 µm)

3.13 Process Economic Study and Cost's Comparison

To better decide on the effectiveness and feasibility of a method and to predict and implement any potential environmental consequences, it is recommended that process costs be estimated taking into account the practicality of the material preparation procedures [122, 123]. These calculations were performed at the laboratory scale and their results, as well as those for other materials previously available in the scientific literature, are presented and summarized in Table 5.

The cost of the raw materials is almost negligible since they are agri-food waste available in large quantities. Therefore, the total cost is dominated by the cost of the chemicals used for the preparation of the two adsorbents. In conclusion, the adsorption of 1 L of methylene blue dye

Table 5 Cost analysis of methylene blue adsorption on TWS and TPS

	Unit price ($ kg^{-1})	Amount of required raw materials in kg for adsorbing 1L of methylene blue (kg L^{-1})	Cost ($ L^{-1})
Natural material			
Walnut shells	0.50	0.0005	0.0003
Peanut shells	0.02	0.0005	0.0000
Chemicals			
Ultrapure water	5.25	0.0100	0.0525
Ethanol (C_2H_5OH, 95%)	6.59	0.0100	0.0659
Hydrogen peroxide (H_2O_2, 30%)	31.24	0.0025	0.0781
Walnut shells treated by chemicals			0.1968
Peanut shells treated by chemicals			0.1965
Energy-consuming during drying at 100 °C for 24 h			0.5000
TWS			0.6968
TPS			0.6965

costs \$0.6968 using walnut shells and \$0.6965 using peanut shells. These two adsorbents remain less expensive overall compared to graphene oxide which costs \$3.31 to synthesize 1 g [124] or to other commercial materials such as activated carbons whose price is around \$0.75 and \$2.60 kg^{-1}, silica gels which cost approximately \$4.4 to \$5.3 kg^{-1}, and polymer beads whose price is around \$5.5 kg^{-1} [125]. Economically, both the two adsorbents TWS and TPS are inexpensive materials for industrial wastewater treatment.

4 Conclusions

The elimination of methylene blue from the aqueous solution by biosorption on the treated walnut shells and the treated peanut shells was studied in the present study. The biosorption capacity was estimated based on the initial pH, the contact time at different initial concentrations of dye, the dose of biosorbent, the temperature of the solution, and particle size. The kinetic modeling study showed that the experimental data followed the pseudo-second-order model. The equilibrium data were better adapted to the Langmuir isotherm model with a maximum mono-layer adsorption capacity of 101.43 mg g^{-1} for treated walnut shells and 67.42 mg g^{-1} for treated peanut shells. Thermodynamic analysis has shown that the adsorption of methylene blue by both treated walnut shells and treated peanut shells powders is a spontaneous, feasible, endothermic, physisorption and that the interfaces between the liquid and solid phases decrease randomly during the process. Treated walnut shells and treated peanut shells, as bio-adsorbents, have great potential for removing textile dyes because these are low-cost products and there is no need for expensive equipment and because of their regeneration power to be reused in the adsorption of methylene blue cationic dye despite the decrease in adsorption capacity up to the fourth cycle of regeneration due to the reduction in specific surface area by heat treatment. Furthermore, the cost analysis revealed that the adsorption of one liter of methylene blue dye costs \$0.6968 with walnut shells and \$0.6965 with peanut shells. Therefore, both TWS and TPS biomaterials could be considered cost-effective, selective, promising, and environmentally friendly for textile dye removal. Last but not least, chemometric tools, such as the design of experiments and artificial neural networks, could be explored in the valorization of peanut shells and walnut shells as effective bio-adsorbents to predict and optimize dyes removal from textile wastewater as an interesting perspective for future work.

Data availability The dataset used during this study is available from the corresponding author on reasonable request.

Declarations

Conflict of interest The authors declared no potential conflict of interest concerning the research, authorship, and/or publication of this article.

References

1. Kalra A, Gupta A (2021) Recent advances in decolourization of dyes using iron nanoparticles: a mini review. Mater Today Proc 36:689–696. https://doi.org/10.1016/j.matpr.2020.04.677
2. Manojlović D, Lelek K, Roglić G, Zherebtsov D, Avdin V, Buskina K, Sakthidharan C, Sapozhnikov S, Samodurova M, Zakirov R, Stanković DM (2020) Efficiency of homely synthesized magnetite: carbon composite anode toward decolorization of reactive textile dyes. Int J Environ Sci Technol 17:2455–2462. https://doi.org/10.1007/s13762-020-02654-8
3. Saratale RG, Rajesh Banu J, Shin H-S, Bharagava RN, Saratale GD (2020) Textile Industry wastewaters as major sources of environmental contamination: bioremediation approaches for its degradation and detoxification. In: Saxena G, Bharagava RN (eds) Bioremediation of industrial waste for environmental safety. Springer Singapore, Singapore, pp 135–167. https://doi.org/10.1007/978-981-13-1891-7_7
4. Akazawa M, Wu Y-H, Liu W-M (2019) Allergy-like reactions to methylene blue following laparoscopic chromopertubation: a systematic review of the literature. Eur J Obstet Gynecol Reprod Biol 238:58–62. https://doi.org/10.1016/j.ejogrb.2019.03.019
5. Balu S, Uma K, Pan G-T, Yang T, Ramaraj S (2018) Degradation of methylene blue dye in the presence of visible light using SiO2@α-Fe2O3 nanocomposites deposited on SnS2 flowers. Materials 11:1030. https://doi.org/10.3390/ma11061030
6. Tkaczyk A, Mitrowska K, Posyniak A (2020) Synthetic organic dyes as contaminants of the aquatic environment and their implications for ecosystems: a review. Sci Total Environ 717:137222. https://doi.org/10.1016/j.scitotenv.2020.137222
7. Al Kindi GY, Gomaa GF, Abd Ulkareem FA (2020) Combined adsorbent best (chemical and natural) coagulation process for removing some heavy metals from wastewater. Int J Environ Sci Technol 17:3431–3448. https://doi.org/10.1007/s13762-020-02702-3
8. Lei Y, Huang Q, Dou J, Huang H, Yang G, Deng F, Liu M, Li X, Zhang X, Wei Y (2021) Fast adsorptive removal of cationic organic dye by anionic group functionalized carbon nanotubes with high efficiency. Colloid Interface Sci Commun 40:100328. https://doi.org/10.1016/j.colcom.2020.100328
9. Luo W, Ying J, Yu S, Yang X, Jia Y, Chen M, Zhang H, Gao J, Li Y, Mai Y-W, Wu Z (2020) ZnS: Cu powders with strong visible-light photocatalysis and pyro-catalysis for room-temperature dye decomposition. Ceram Int 46:12096–12101. https://doi.org/10.1016/j.ceramint.2020.01.253
10. Miyah Y, Lahrichi A, Kachkoul R, El Mouhri G, Idrissi M, Iaich S, Zerrouq F (2020) Multi-parametric filtration effect of the dyes mixture removal with the low cost materials. Arab J Basic Appl Sci 27:248–258. https://doi.org/10.1080/25765299.2020.1776008
11. Onga L, Kornev I, Preis S (2020) Oxidation of reactive azo-dyes with pulsed corona discharge: Surface reaction enhancement. J Electrostat 103:103420. https://doi.org/10.1016/j.elstat.2020.103420
12. Grace Pavithra K, Senthil KP, Jaikumar V, Sundar Rajan P (2019) Removal of colorants from wastewater: a review on sources and

treatment strategies. J Ind Eng Chem 75:1–19. https://doi.org/10.1016/j.jiec.2019.02.011
13. Jain M, Khan SA, Pandey A, Pant KK, Ziora ZM, Blaskovich MAT (2021) Instructive analysis of engineered carbon materials for potential application in water and wastewater treatment. Sci Total Environ 793:148583. https://doi.org/10.1016/j.scitotenv.2021.148583
14. Jawad AH, Malek NNA, Abdulhameed AS, Razuan R (2020) Synthesis of magnetic chitosan-Fly Ash/Fe3O4 composite for adsorption of reactive orange 16 dye: optimization by box-behnken design. J Polym Environ 28:1068–1082. https://doi.org/10.1007/s10924-020-01669-z
15. Malek NNA, Jawad AH, Abdulhameed AS, Ismail K, Hameed BH (2020) New magnetic Schiff's base-chitosan-glyoxal/fly ash/Fe3O4 biocomposite for the removal of anionic azo dye: an optimized process. Int J Biol Macromol 146:530–539. https://doi.org/10.1016/j.ijbiomac.2020.01.020
16. Sri Devi V, Sudhakar B, Prasad K, Jeremiah Sunadh P, Krishna M (2020) Adsorption of Congo red from aqueous solution onto Antigonon leptopus leaf powder: equilibrium and kinetic modeling. Mater Today Proc. 26:3197–3206. https://doi.org/10.1016/j.matpr.2020.02.715
17. Miyah Y, Benjelloun M, Lahrichi A, Mejbar F, Iaich S, El Mouhri G, Kachkoul R, Zerrouq F (2021) Highly-efficient treated oil shale ash adsorbent for toxic dyes removal: kinetics, isotherms, regeneration, cost analysis and optimization by experimental design. J Environ Chem Eng 9:106694. https://doi.org/10.1016/j.jece.2021.106694
18. Koyuncu H, Kul AR (2020) Biosorption study for removal of methylene blue dye from aqueous solution using a novel activated carbon obtained from nonliving lichen (*Pseudevernia furfuracea* (L.) Zopf.). Surf Interfaces. https://doi.org/10.1016/j.surfin.2020.100527
19. Öztürk A, Bayol E, Abdullah MI (2020) Characterization of the biosorption of fast black azo dye K salt by the bacterium *Rhodopseudomonas palustris* 51ATA strain. Electron J Biotechnol 46:22–29. https://doi.org/10.1016/j.ejbt.2020.05.002
20. Tukaram Bai M, Shaik O, Kavitha J, Hemanth Varma MS, Chittibabu N (2020) Biosorption of eosin yellow dye from aqueous solution using sugarcane bagasse: equillibrium, kinetics and thermodynamics. Mater Today Proc. 26:842–849. https://doi.org/10.1016/j.matpr.2020.01.051
21. Arab C, El Kurdi R, Patra D (2022) Zinc curcumin oxide nanoparticles for enhanced adsorption of Congo red: kinetics and adsorption isotherms study. Mater Today Chem 23:100701. https://doi.org/10.1016/j.mtchem.2021.100701
22. Siraorarnroj S, Kaewtrakulchai N, Fuji M, Eiad-ua A (2022) High performance nanoporous carbon from mulberry leaves (Morus alba L) residues via microwave treatment assisted hydrothermal-carbonization for methyl orange adsorption: kinetic, equilibrium and thermodynamic studies. Materialia 21:101288. https://doi.org/10.1016/j.mtla.2021.101288
23. Karaman C, Karaman O, Show P-L, Karimi-Maleh H, Zare N (2022) Congo red dye removal from aqueous environment by cationic surfactant modified-biomass derived carbon: equilibrium, kinetic, and thermodynamic modeling, and forecasting via artificial neural network approach. Chemosphere 290:133346. https://doi.org/10.1016/j.chemosphere.2021.133346
24. Amar IA, Zayid EA, Dhikeel SA, Najem MY (2021) Biosorption removal of methylene blue dye from aqueous solutions using phosphoric acid-treated balanites aegyptiaca seed husks powder. Biointerface Res Appl Chem. 12:7845–7862. https://doi.org/10.33263/BRIAC126.78457862
25. Uddin MdT, Rahman MdA, Rukanuzzaman Md, Islam MdA (2017) A potential low cost adsorbent for the removal of cationic dyes from aqueous solutions. Appl Water Sci 7:2831–2842. https://doi.org/10.1007/s13201-017-0542-4
26. Carvalho LB, Chagas PMB, Pinto LMA (2018) Caesalpinia ferrea Fruits as a Biosorbent for the Removal of Methylene Blue Dye from an Aqueous Medium. Water Air Soil Pollut 229:297. https://doi.org/10.1007/s11270-018-3952-5
27. Oyebamiji OO, Boeing WJ, Holguin FO, Ilori O, Amund O (2019) Green microalgae cultured in textile wastewater for biomass generation and biodetoxification of heavy metals and chromogenic substances. Bioresource Technology Reports 7:100247. https://doi.org/10.1016/j.biteb.2019.100247
28. Garg D, Kumar S, Sharma K, Majumder CB (2019) Application of waste peanut shells to form activated carbon and its utilization for the removal of Acid Yellow 36 from wastewater, Groundwater for. Sustain Dev 8:512–519. https://doi.org/10.1016/j.gsd.2019.01.010
29. Garg D, Majumder CB, Kumar S, Sarkar B (2019) Removal of Direct Blue-86 dye from aqueous solution using alginate encapsulated activated carbon (PnsAC-alginate) prepared from waste peanut shell. J Environ Chem Eng 7:103365. https://doi.org/10.1016/j.jece.2019.103365
30. Liu J, Wang Z, Li H, Hu C, Raymer P, Huang Q (2018) Effect of solid state fermentation of peanut shell on its dye adsorption performance. Biores Technol 249:307–314. https://doi.org/10.1016/j.biortech.2017.10.010
31. Hajialigol S, Masoum S (2019) Optimization of biosorption potential of nano biomass derived from walnut shell for the removal of Malachite Green from liquids solution: Experimental design approaches. J Mol Liq 286:110904. https://doi.org/10.1016/j.molliq.2019.110904
32. X. Pang, L. Sellaoui, D. Franco, G.L. Dotto, J. Georgin, A. Bajahzar, H. Belmabrouk, A. Ben Lamine, A. Bonilla-Petriciolet, Z. Li, Adsorption of crystal violet on biomasses from pecan nutshell, para chestnut husk, araucaria bark and palm cactus: Experimental study and theoretical modeling via monolayer and double layer statistical physics models, Chemical Engineering Journal. 378 (2019) 122101. https://doi.org/10.1016/j.cej.2019.122101.
33. Bouteiba A, Benhadria N, Elaziouti A, Ezziane K, Bettahar N (2020) Competitive adsorption of binary dye from aqueous solutions using calcined layered double hydroxides. Int J Environ Anal Chem. https://doi.org/10.1080/03067319.2020.1766035
34. Hayoun B, Bourouina M, Pazos M, Sanromán MA, Bourouina-Bacha S (2020) Equilibrium Study, Modeling and Optimization of Model Drug Adsorption Process by Sunflower Seed Shells. Appl Sci 10:3271. https://doi.org/10.3390/app10093271
35. Hui TS, Zaini MAA (2021) Valorization of spent activated carbon in glycerine deodorization unit for methylene blue removal. Carbon Letters 31:721–728. https://doi.org/10.1007/s42823-020-00189-z
36. Melhaoui R, Miyah Y, Kodad S, Houmy N, Addi M, Abid M, Mihamou A, Serghini-Caid H, Lairini S, Tijani N, Hano C, Elamrani A (2021) On the Suitability of Almond Shells for the Manufacture of a Natural Low-Cost Bioadsorbent to Remove Brilliant Green: Kinetics and Equilibrium Isotherms Study. Sci World J 2021:1–13. https://doi.org/10.1155/2021/6659902
37. Yao X, Ji L, Guo J, Ge S, Lu W, Cai L, Wang Y, Song W, Zhang H (2020) Magnetic activated biochar nanocomposites derived from wakame and its application in methylene blue adsorption. Biores Technol 302:122842. https://doi.org/10.1016/j.biortech.2020.122842
38. Loulidi I, Boukhlifi F, Ouchabi M, Amar A, Jabri M, Kali A, Chraibi S (2019) Adsorptive removal of chromium (VI) using walnut shell almond shell, coconut shell and peanut shell. Res J Chem Environ 23:25–32

39. Xue H, Wang X, Xu Q, Dhaouadi F, Sellaoui L, Seliem MK, Ben Lamine A, Belmabrouk H, Bajahzar A, Bonilla-Petriciolet A, Li Z, Li Q (2022) Adsorption of methylene blue from aqueous solution on activated carbons and composite prepared from an agricultural waste biomass: a comparative study by experimental and advanced modeling analysis. Chem Eng J 430:132801. https://doi.org/10.1016/j.cej.2021.132801
40. Das A, Banerjee M, Bar N, Das SK (2019) Adsorptive removal of Cr(VI) from aqueous solution: kinetic, isotherm, thermodynamics, toxicity, scale-up design, and GA modeling. SN Appl Sci 1:776. https://doi.org/10.1007/s42452-019-0813-9
41. Horikawa Y, Hirano S, Mihashi A, Kobayashi Y, Zhai S, Sugiyama J (2019) Prediction of lignin contents from infrared spectroscopy: chemical digestion and lignin/biomass ratios of *Cryptomeria japonica*. Appl Biochem Biotechnol 188:1066–1076. https://doi.org/10.1007/s12010-019-02965-8
42. Moosavinejad SM, Madhoushi M, Vakili M, Rasouli D (2019) Evaluation of degradation in chemical compounds of wood in historical buildings using FT-IR and FT-Raman vibrational spectroscopy, Maderas. Cienc Tecn 21:381–392. https://doi.org/10.4067/S0718-221X2019005000310
43. Uddin MK, Nasar A (2020) Walnut shell powder as a low-cost adsorbent for methylene blue dye: isotherm, kinetics, thermodynamic, desorption and response surface methodology examinations. Sci Rep 10:7983. https://doi.org/10.1038/s41598-020-64745-3
44. Dias M, Pinto J, Henriques B, Figueira P, Fabre E, Tavares D, Vale C, Pereira E (2021) Nutshells as Efficient biosorbents to remove cadmium, lead, and mercury from contaminated solutions. Int J Environ Res Public Health 18:1580. https://doi.org/10.3390/ijerph18041580
45. Georgieva VG, Gonsalvesh L, Tavlieva MP (2020) Thermodynamics and kinetics of the removal of nickel (II) ions from aqueous solutions by biochar adsorbent made from agro-waste walnut shells. J Mol Liq. https://doi.org/10.1016/j.molliq.2020.112788
46. Ojo TA, Ojedokun AT, Bello OS (2019) Functionalization of powdered walnut shell with orthophosphoric acid for Congo red dye removal. Part Sci Technol 37:74–85. https://doi.org/10.1080/02726351.2017.1340914
47. Liu X, Xu X, Dong X, Park J (2020) Competitive adsorption of heavy metal ions from aqueous solutions onto activated carbon and agricultural waste materials. Polish J Environ Stud. 29:749–761. https://doi.org/10.15244/pjoes/104455
48. Qiu Z, Wang M, Zhang T, Yang D, Qiu F (2020) In-situ fabrication of dynamic and recyclable TiO2 coated bacterial cellulose membranes as an efficient hybrid absorbent for tellurium extraction. Cellulose 27:4591–4608. https://doi.org/10.1007/s10570-020-03096-8
49. El Mouhri G, Merzouki M, Belhassan H, Miyah Y, Amakdouf H, Elmountassir R, Lahrichi A (2020) Continuous adsorption modeling and fixed bed column studies: adsorption of tannery wastewater pollutants using beach sand. J Chem 2020:1–9. https://doi.org/10.1155/2020/7613484
50. Zhao B, Ren L, Du Y, Wang J (2020) Eco-friendly separation layers based on waste peanut shell for gravity-driven water-in-oil emulsion separation. J Clean Prod 255:120184. https://doi.org/10.1016/j.jclepro.2020.120184
51. Zbair M, Bottlinger M, Ainassaari K, Ojala S, Stein O, Keiski RL, Bensitel M, Brahmi R (2020) Hydrothermal carbonization of argan nut shell: functional mesoporous carbon with excellent performance in the adsorption of bisphenol A and diuron. Waste Biomass Valorization 11:1565–1584. https://doi.org/10.1007/s12649-018-00554-0
52. Jakob M, Mahendran AR, Gindl-Altmutter W, Bliem P, Konnerth J, Müller U, Veigel S (2022) The strength and stiffness of oriented wood and cellulose-fibre materials: a review. Prog Mater Sci 125:100916. https://doi.org/10.1016/j.pmatsci.2021.100916
53. Yusmaniar Y, Erdawati E, Ghifari YF, Ubit DP (2020) Synthesis of mesopore silica composite from rice husk with activated carbon from coconut shell as absorbent methyl orange color adsorbent. IOP Conf Ser Mater Sci Eng. https://doi.org/10.1088/1757-899X/830/3/032078
54. Li J, Zhang J, Natarajan H, Zhang J, Ashok B, Rajulu Anumakonda V (2019) Modification of agricultural waste tamarind fruit shell powder by *in situ* generation of silver nanoparticles for antibacterial filler applications. Int J Polym Anal Charact 24:421–427. https://doi.org/10.1080/1023666X.2019.1602319
55. Amo-Duodu G, Tetteh EK, Rathilal S, Armah EK, Adedeji J, Chollom MN, Chetty M (2021) Effect of engineered biomaterials and magnetite on wastewater treatment: biogas and kinetic evaluation. Polymers 13:4323. https://doi.org/10.3390/polym13244323
56. Miyah Y, Lahrichi A, Idrissi M, Boujraf S, Taouda H, Zerrouq F (2017) Assessment of adsorption kinetics for removal potential of Crystal Violet dye from aqueous solutions using Moroccan pyrophyllite. J Assoc Arab Univ Basic Appl Sci 23:20–28. https://doi.org/10.1016/j.jaubas.2016.06.001
57. Dakhil I, Naser G, Ali A (2021) Assessment of modified rice husks for removal of aniline in batch adsorption process: optimization and isotherm study. J Ecol Eng. 22:179–189. https://doi.org/10.12911/22998993/138900
58. Jawad AH, Abdulhameed AS (2020) Mesoporous Iraqi red kaolin clay as an efficient adsorbent for methylene blue dye: adsorption kinetic, isotherm and mechanism study. Surfaces Interfaces 18:100422. https://doi.org/10.1016/j.surfin.2019.100422
59. Nahali L, Miyah Y, Assila O, EL Badraoui A, EL Khazzan B, Zerrouq F (2019) Kinetic and thermodynamic study of the adsorption of twodyes:brilliant green and eriochrome black T using a natural adsorbent "sugarcane bagasse"., Moroccan. J Chem 7:715–726
60. Bensalah H, Younssi SA, Ouammou M, Gurlo A, Bekheet MF (2020) Azo dye adsorption on an industrial waste-transformed hydroxyapatite adsorbent: Kinetics, isotherms, mechanism and regeneration studies. J Environ Chem Eng 8:103807. https://doi.org/10.1016/j.jece.2020.103807
61. Zou J, Liao K, Xiang L, Liu M, Xie F, Liu X, Yu J, An X, Wang Y (2020) Synthesis of Poly(cyclotriphosphazene-co-4,4′-diaminodiphenysulfone) microspheres and their adsorption properties for cationic dyes (methylene blue). J Inorg Organomet Polym Mater 30:976–985. https://doi.org/10.1007/s10904-019-01235-8
62. El mouhri G, Merzouki M, Kachkoul R, Belhassan H, Miyah Y, Amakdouf H, Elmountassir R, Lahrichi A (2021) Fixed-bed adsorption of tannery wastewater pollutants using bottom ash: An optimized process. Surf Interfaces 22:100868. https://doi.org/10.1016/j.surfin.2020.100868
63. Hevira L, Rahmayeni Z, Ighalo JO, Zein R (2020) Biosorption of indigo carmine from aqueous solution by Terminalia Catappa shell. J Environ Chem Eng 8:104290. https://doi.org/10.1016/j.jece.2020.104290
64. Mok CF, Ching YC, Muhamad F, Abu Osman NA, Hai ND, Che Hassan CR (2020) Adsorption of dyes using poly(vinyl alcohol) (PVA) and PVA-based polymer composite adsorbents: a review. J Polym Environ 28:775–793. https://doi.org/10.1007/s10924-020-01656-4
65. Sakr F, Alahiane S, Sennaoui A, Dinne M, Bakas I, Assabbane A (2020) Removal of cationic dye (Methylene Blue) from aqueous solution by adsorption on two type of biomaterial of South Morocco. Materials Today: Proceedings 22:93–96. https://doi.org/10.1016/j.matpr.2019.08.101

66. Ambaye TG, Vaccari M, van Hullebusch ED, Amrane A, Rtimi S (2021) Mechanisms and adsorption capacities of biochar for the removal of organic and inorganic pollutants from industrial wastewater. Int J Environ Sci Technol 18:3273–3294. https://doi.org/10.1007/s13762-020-03060-w
67. Mejbar F, Miyah Y, EL Badraoui A, Nahali L, Ouissal A, Khalil A, Zerrouq F (2019) Studies of the adsorption kinetics process for removal of methylene blue dye by residue of grenadine bark extraction, Moroccan. J Chem 6:436–443
68. Akl MA, Youssef AFM, Hassan AH, Maher H (2016) Synthesis, characterization and evaluation of peanut shells-derived activated carbons for removal of methomyl from aqueous solutions. J Environ Anal Toxicol 6:352. https://doi.org/10.4172/2161-0525.1000352
69. Bayes GS, Raut SS, Patil VR, Lokhande RS (2012) Formation of diazepam–lanthanides(III) complexes in the 50–50 volume % ethanol-water solvent system and study of the effect of temperature on the complex formation constants. J Solution Chem 41:241–248. https://doi.org/10.1007/s10953-012-9798-3
70. Miyah Y, Lahrichi A, Idrissi M, Khalil A, Zerrouq F (2018) Adsorption of methylene blue dye from aqueous solutions onto walnut shells powder: Equilibrium and kinetic studies. Surf Interfaces 11:74–81. https://doi.org/10.1016/j.surfin.2018.03.006
71. Biswas S, Sen TK, Yeneneh AM, Meikap BC (2019) Synthesis and characterization of a novel Ca-alginate-biochar composite as efficient zinc (Zn^{2+}) adsorbent: thermodynamics, process design, mass transfer and isotherm modeling. Sep Sci Technol 54:1106–1124. https://doi.org/10.1080/01496395.2018.1527353
72. Alver E, Metin AÜ, Brouers F (2020) Methylene blue adsorption on magnetic alginate/rice husk bio-composite. Int J Biol Macromol 154:104–113. https://doi.org/10.1016/j.ijbiomac.2020.02.330
73. Mosoarca G, Vancea C, Popa S, Gheju M, Boran S (2020) Syringa vulgaris leaves powder a novel low-cost adsorbent for methylene blue removal: isotherms, kinetics, thermodynamic and optimization by Taguchi method. Sci Rep 10:17676. https://doi.org/10.1038/s41598-020-74819-x
74. de Silva CEF, da Gama BMV, da Gonçalves AHS, Medeiros JA, de Abud AKS (2020) Basic-dye adsorption in albedo residue: effect of pH, contact time, temperature, dye concentration, biomass dosage, rotation and ionic strength. J King Saud Univ Eng Sci. 32:351–359. https://doi.org/10.1016/j.jksues.2019.04.006
75. Zhao X, Chen Y (2020) Adsorption of methylene blue using FeCl3-modified pomelo peel. Russ J Phys Chem A 94:835–845. https://doi.org/10.1134/S0036024420040263
76. Batool F, Akbar J, Iqbal S, Noreen S, Bukhari SNA (2018) Study of isothermal, kinetic, and thermodynamic parameters for adsorption of cadmium: an overview of linear and nonlinear approach and error analysis. Bioinorg Chem Appl 2018:1–11. https://doi.org/10.1155/2018/3463724
77. Dahdouh N, Amokrane S, Murillo R, Mekatel E, Nibou D (2020) Removal of methylene blue and basic yellow 28 dyes from aqueous solutions using sulphonated waste poly methyl methacrylate. J Polym Environ 28:271–283. https://doi.org/10.1007/s10924-019-01605-w
78. Kankılıç GB, Metin AÜ (2020) Phragmites australis as a new cellulose source: extraction, characterization and adsorption of methylene blue. J Mol Liq. https://doi.org/10.1016/j.molliq.2020.113313
79. Karoui S, Ben Arfi R, Mougin K, Ghorbal A, Assadi AA, Amrane A (2020) Synthesis of novel biocomposite powder for simultaneous removal of hazardous ciprofloxacin and methylene blue: central composite design, kinetic and isotherm studies using Brouers-Sotolongo family models. J Hazard Mater 387:121675. https://doi.org/10.1016/j.jhazmat.2019.121675
80. Soltani R, Marjani A, Shirazian S (2019) Facile one-pot synthesis of thiol-functionalized mesoporous silica submicrospheres for Tl(I) adsorption: Isotherm, kinetic and thermodynamic studies. J Hazard Mater 371:146–155. https://doi.org/10.1016/j.jhazmat.2019.02.076
81. Wang J, Gao M, Shen T, Yu M, Xiang Y, Liu J (2019) Insights into the efficient adsorption of rhodamine B on tunable organo-vermiculites. J Hazard Mater 366:501–511. https://doi.org/10.1016/j.jhazmat.2018.12.031
82. Benjelloun M, Miyah Y, Akdemir Evrendilek G, Zerrouq F, Lairini S (2021) Recent advances in adsorption kinetic models: their application to dye types. Arab J Chem 14:103031. https://doi.org/10.1016/j.arabjc.2021.103031
83. Langmuir I (1918) The adsorption of gases on plane surfaces of glass, mica and platinum. J Am Chem Soc 40:1361–1403. https://doi.org/10.1021/ja02242a004
84. Yurekli Y (2019) Determination of adsorption characteristics of synthetic NaX nanoparticles. J Hazard Mater 378:120743. https://doi.org/10.1016/j.jhazmat.2019.120743
85. Mahmoodi NM, Arami M (2008) Modeling and sensitivity analysis of dyes adsorption onto natural adsorbent from colored textile wastewater. J Appl Polym Sci 109:4043–4048. https://doi.org/10.1002/app.28547
86. Itodo AU, Itodo HU, Gafar MK (2010) Estimation of specific surface area using Langmuir isotherm method. J Appl Sci Environ Manag 14:141–145
87. Fahoul Y, Zouheir M, Tanji K, Kherbeche A (2022) Synthesis of a novel ZnAl2O4/CuS nanocomposite and its characterization for photocatalytic degradation of acid red 1 under UV illumination. J Alloy Compd 889:161708. https://doi.org/10.1016/j.jallcom.2021.161708
88. Freundlich H (1907) Über die Adsorption in Lösungen. Zeitschrift für Physikalische Chemie (Leipzig) 57U:385–470. https://doi.org/10.1515/zpch-1907-5723
89. Othman NH, Alias NH, Shahruddin MZ, Abu Bakar NF, Nik Him NR, Lau WJ (2018) Adsorption kinetics of methylene blue dyes onto magnetic graphene oxide. J Environ Chem Eng 6:2803–2811. https://doi.org/10.1016/j.jece.2018.04.024
90. Dubinin MM (1960) The potential theory of adsorption of gases and vapors for adsorbents with energetically nonuniform surfaces. Chem Rev 60:235–241. https://doi.org/10.1021/cr60204a006
91. Haul R, Gregg SJ, Sing KSW (1982) Adsorption, Surface Area and Porosity. 2. Auflage, Academic Press, London 1982. 303 Seiten, Preis: $ 49.50. Ber Bunsenges Phys Chem 86:957–957. https://doi.org/10.1002/bbpc.19820861019
92. Hutson ND, Yang RT (1997) Theoretical basis for the Dubinin-Radushkevitch (D-R) adsorption isotherm equation. Adsorption 3:189–195. https://doi.org/10.1007/BF01650130
93. Tang X, Ran G, Li J, Zhang Z, Xiang C (2021) Extremely efficient and rapidly adsorb methylene blue using porous adsorbent prepared from waste paper: Kinetics and equilibrium studies. J Hazard Mater 402:123579. https://doi.org/10.1016/j.jhazmat.2020.123579
94. Inglezakis VJ (2007) Solubility-normalized Dubinin-Astakhov adsorption isotherm for ion-exchange systems. Microporous Mesoporous Mater 103:72–81. https://doi.org/10.1016/j.micromeso.2007.01.039
95. Hu Q, Zhang Z (2019) Application of Dubinin-Radushkevich isotherm model at the solid/solution interface: a theoretical analysis. J Mol Liq 277:646–648. https://doi.org/10.1016/j.molliq.2019.01.005
96. Al-Wabel MI, Ahmad M, Usman ARA, Sallam AS, Hussain Q, Binyameen RB, Shehu MR, Ok YS (2020) Evaluating the efficiency of different natural clay sediments for the removal

of chlortetracycline from aqueous solutions. J Hazard Mater 384:121500. https://doi.org/10.1016/j.jhazmat.2019.121500
97. Low SK, Tan MC (2018) Dye adsorption characteristic of ultrasound pre-treated pomelo peel. J Environ Chem Eng 6:3502–3509. https://doi.org/10.1016/j.jece.2018.05.013
98. Jawad AH, Mubarak NSA, Abdulhameed AS (2020) Hybrid crosslinked Chitosan-Epichlorohydrin/TiO2 nanocomposite for reactive red 120 dye adsorption: kinetic, isotherm, thermodynamic, and mechanism study. J Polym Environ 28:624–637. https://doi.org/10.1007/s10924-019-01631-8
99. Lach J, Ociepa-Kubicka A, Mrowiec M (2021) Oxytetracycline adsorption from aqueous solutions on commercial and high-temperature modified activated carbons. Energies 14:3481. https://doi.org/10.3390/en14123481
100. Mohammad A-T, Abdulhameed AS, Jawad AH (2019) Box-Behnken design to optimize the synthesis of new crosslinked chitosan-glyoxal/TiO2 nanocomposite: methyl orange adsorption and mechanism studies. Int J Biol Macromol 129:98–109. https://doi.org/10.1016/j.ijbiomac.2019.02.025
101. Rodrigues AE, Silva CM (2016) What's wrong with Lagergreen pseudo first order model for adsorption kinetics? Chem Eng J 306:1138–1142. https://doi.org/10.1016/j.cej.2016.08.055
102. Moussout H, Ahlafi H, Aazza M, Maghat H (2018) Critical of linear and nonlinear equations of pseudo-first order and pseudo-second order kinetic models. Karbala Int J Modern Sci 4:244–254. https://doi.org/10.1016/j.kijoms.2018.04.001
103. Marco-Brown JL, Guz L, Olivelli MS, Schampera B, Torres Sánchez RM, Curutchet G, Candal R (2018) New insights on crystal violet dye adsorption on montmorillonite: kinetics and surface complexes studies. Chem Eng J 333:495–504. https://doi.org/10.1016/j.cej.2017.09.172
104. Plazinski W, Dziuba J, Rudzinski W (2013) Modeling of sorption kinetics: the pseudo-second order equation and the sorbate intraparticle diffusivity. Adsorption 19:1055–1064. https://doi.org/10.1007/s10450-013-9529-0
105. Rout S, Kumar A, Ravi PM, Tripathi RM (2015) Pseudo second order kinetic model for the sorption of U (VI) onto soil: a comparison of linear and non-linear methods. Int J Environ Sci 6:145–154. https://doi.org/10.6088/ijes.6017
106. Weber WJ, Morris JC (1963) Kinetics of adsorption on carbon from solution. J Sanit Eng Div 89:31–60
107. Jiang C, Wang X, Qin D, Da W, Hou B, Hao C, Wu J (2019) Construction of magnetic lignin-based adsorbent and its adsorption properties for dyes. J Hazard Mater 369:50–61. https://doi.org/10.1016/j.jhazmat.2019.02.021
108. Mane VS, Deo Mall I, Chandra Srivastava V (2007) Kinetic and equilibrium isotherm studies for the adsorptive removal of Brilliant Green dye from aqueous solution by rice husk ash. J Environ Manag 84:390–400. https://doi.org/10.1016/j.jenvman.2006.06.024
109. Mohanty K, Das D, Biswas MN (2005) Adsorption of phenol from aqueous solutions using activated carbons prepared from Tectona grandis sawdust by ZnCl2 activation. Chem Eng J 115:121–131. https://doi.org/10.1016/j.cej.2005.09.016
110. Al-Aoh HA, Aljohani MMH, Darwish AAA, Ayaz Ahmad M, Bani-Atta SA, Alsharif MA, Mahrous YM, Mustafa SK, Al-Shehri HS, Alrawashdeh LR, Al-Tweher JN (2021) A potentially low-cost adsorbent for Methylene Blue removal from synthetic wastewater. Desalination Water Treat. 213:431–440. https://doi.org/10.5004/dwt.2021.26732
111. Alizadeh N, Shariati S, Besharati N (2017) Adsorption of crystal violet and methylene blue on azolla and fig leaves modified with magnetite iron oxide nanoparticles. Int J Environ Res 11:197–206. https://doi.org/10.1007/s41742-017-0019-1
112. Dra A, Tanji K, Arrahli A, Iboustaten EM, El Gaidoumi A, Kherchafi A, Benabdallah AC, Kherbeche A (2020) Valorization of Oued Sebou Natural Sediments (Fez-Morocco Area) as adsorbent of methylene blue dye: kinetic and thermodynamic study. Sci World J 2020:1–8. https://doi.org/10.1155/2020/2187129
113. Ghosh I, Kar S, Chatterjee T, Bar N, Das SK (2021) Removal of methylene blue from aqueous solution using Lathyrus sativus husk: adsorption study, MPR and ANN modelling. Process Saf Environ Prot 149:345–361. https://doi.org/10.1016/j.psep.2020.11.003
114. Islam T, Hyder AG, Saenz-Arana R, Hernandez C, Guinto T, Ahsan A, Alvarado-Tenorio B, Noveron JC (2019) Derived adsorbent prepared by sulfuric acid reflux. J Environ Chem Eng 7:1–12. https://doi.org/10.1016/j.jece.2018.102816
115. Jawad AH, Abdulhameed AS, Mastuli MS (2020) Acid-factionalized biomass material for methylene blue dye removal: a comprehensive adsorption and mechanism study. J Taibah Univ Sci 14:305–313. https://doi.org/10.1080/16583655.2020.1736767
116. Mishra SP, Patra AR, Das S (2020) Methylene blue and malachite green removal from aqueous solution using waste activated carbon. Biointerface Res Appl Chem. 11:7410–7421. https://doi.org/10.33263/BRIAC111.74107421
117. Shooto ND, Thabede PM, Bhila B, Moloto H, Naidoo EB (2020) Lead ions and methylene blue dye removal from aqueous solution by mucuna beans (velvet beans) adsorbents. J Environ Chem Eng 8:103557. https://doi.org/10.1016/j.jece.2019.103557
118. Siddiqui SI, Rathi G, Chaudhry SA (2018) Acid washed black cumin seed powder preparation for adsorption of methylene blue dye from aqueous solution: thermodynamic, kinetic and isotherm studies. J Mol Liq 264:275–284. https://doi.org/10.1016/j.molliq.2018.05.065
119. Tang Y, Lin T, Jiang C, Zhao Y, Ai S (2021) Renewable adsorbents from carboxylate-modified agro-forestry residues for efficient removal of methylene blue dye. J Phys Chem Solids 149:109811. https://doi.org/10.1016/j.jpcs.2020.109811
120. Aguedal H, Iddou A, Aziz A, Shishkin A, Locs J, Juhna T (2018) Effect of thermal regeneration of diatomite adsorbent on its efficacy for removal of dye from water. Int J Environ Sci Technol. https://doi.org/10.1007/s13762-018-1647-5
121. Antonelli R, Malpass GRP, da Silva MGC, Vieira MGA (2020) Adsorption of ciprofloxacin onto thermally modified bentonite clay: experimental design, characterization, and adsorbent regeneration. J Environ Chem Eng 8:104553. https://doi.org/10.1016/j.jece.2020.104553
122. Al-Absi RS, Abu-Dieyeh MH, Ben-Hamadou R, Nasser MS, Al-Ghouti MA (2022) Thermodynamics, isotherms, and mechanisms studies of lithium recovery from seawater desalination reverse osmosis brine using roasted and ferrocyanide modified date pits. Environ Technol Innov 25:102148. https://doi.org/10.1016/j.eti.2021.102148
123. Suhan MBK, Mahtab SMT, Aziz W, Akter S, Islam MS (2021) Sudan black B dye degradation in aqueous solution by Fenton oxidation process: kinetics and cost analysis. Case Stud Chem Environ Eng 4:100126. https://doi.org/10.1016/j.cscee.2021.100126
124. Rathour RKS, Bhattacharya J (2018) A green approach for single-pot synthesis of graphene oxide and its composite with Mn3O4. Appl Surf Sci 437:41–50. https://doi.org/10.1016/j.apsusc.2017.12.139
125. Andreas A, Winata ZG, Santoso SP, Angkawijaya AE, Yuliana M, Soetaredjo FE, Ismadji S, Hsu H-Y, Go AW, Ju Y-H (2021) Biocomposite hydrogel beads from glutaraldehyde-crosslinked phytochemicals in alginate for effective removal of methylene blue. J Mol Liq 329:115579. https://doi.org/10.1016/j.molliq.2021.115579